

UNIVERSITY OF AMSTERDAM

MASTERS THESIS

Mathematically Modeling the Interactions Between Phages, Bacteria, and the Environment

Author:

Victor PIASKOWSKI

Examiner:

Dr. Jaap Kaandorp

Supervisor:

Dr. Matti Gralka

Assessor:

Dr. Yuval Mulla

*A thesis submitted in partial fulfillment of the requirements
for the degree of Master of Science in Computational Science*

in the

Computational Science Lab
Informatics Institute

June 2025

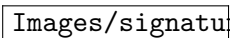
clslogo.png

Declaration of Authorship

I, Victor PIASKOWSKI, declare that this thesis, entitled ‘Mathematically Modeling the Interactions Between Phages, Bacteria, and the Environment’ and the work presented in it are my own. I confirm that:

- This work was done wholly or mainly while in candidature for a research degree at the University of Amsterdam.
- Where any part of this thesis has previously been submitted for a degree or any other qualification at this University or any other institution, this has been clearly stated.
- Where I have consulted the published work of others, this is always clearly attributed.
- Where I have quoted from the work of others, the source is always given. With the exception of such quotations, this thesis is entirely my own work.
- I have acknowledged all main sources of help.
- Where the thesis is based on work done by myself jointly with others, I have made clear exactly what was done by others and what I have contributed myself.

Signed:

re.pdf

Date: June 13, 2025

“All models are wrong, but some are useful”

George E. P. Box

UNIVERSITY OF AMSTERDAM

Abstract

Faculty of Science
Informatics Institute

Master of Science in Computational Science

**Mathematically Modeling the Interactions Between Phages, Bacteria, and
the Environment**

by Victor PIASKOWSKI

The interactions between phages, bacteria, resources, and the environment are complex. Not much is known about how phages interact with bacteria and their surroundings. There is a need to mathematically model phage and bacteria populations, but current models can only model 1 or 2 phages, bacteria strains, and resources. In the marine ecosystem, there can be hundreds of different phages and bacteria interacting with one another. These individual interactions have a greater implication on the ecosystem. Phages have been shown to influence bacteria's population fitness levels by introducing mutations and forcing bacteria to adapt to external stressors. Phages have also been shown to influence the resource recycling process. Upon lysing, bacteria release resources into the environment that other bacteria, plants, and animals can use.

I created a program to create a tool that will create a network representation of the model's interactions. The graph network stores interactions and model parameters such as initial population and reaction rates, as well as environmental conditions like temperature and pH. I also created a simulation framework that can mathematically model the phage, bacteria, and resource population with the provided network, with a user-provided ODE model. The user can interact with the framework with a custom-built dashboard. Using the tools, a user can upload a self-implemented ODE model and network model to a dashboard and a self-implemented ODE model and interactively run simulations on the model. The user can, for example, change the initial resource concentration or how fast a phage infects a bacterium from the dashboard and immediately see how the change affects the simulation. The user can interact with five prebuilt plots. The user can run the simulations and save the results to their disk to create their own custom analyses and plots.

Finally, I analyze a model using the Golding model from Mulla et al. [1]. I qualitatively analyze the model's behavior and use a SOBOL analyses to help assign a quantitative value to the model's behavior. By varying the initial uninfected bacteria population, the model can become adsorption or latency limited. Knowing if a phage population will proliferate in a laboratory context while facing constant washout is important to ensure that the phage population is not wiped out. Given the context of large communities, knowing if phages and bacteria can coexist under various conditions is important, so a co-existence analysis is done and analyzed.

Acknowledgements

I would like to thank my parents for loving me despite some of my faults, and for supporting me through my Bachelor and Master studies even if they don't exactly know what I am studying. Without them, I wouldn't know where my life would be right now, and I certainly would be a different person if it were not for them.

Thank you to Dr. Matti Gralka for the weekly meetings and teaching me everything about phages and bacteria. Every meeting was always insightful, productive, and informative. I will forever be amazed at how he can remember which paper talks about which topic, and how he always had a paper for every topic.

Thank you to Sofia Blaszczyk for finding the Master thesis opening and suggesting that I email Dr. Gralka for an introductory meeting. She acted as my rubber duck programming buddy, and watched my cringe screen recordings that I sent her at 2am showcasing various demos of my project. If she wouldn't have found this opening, I wouldn't know what I would be doing as my thesis.

If I hadn't followed Dr. Rik Kaasschieter's and Dr. Martijn Anthonissen's courses "Introduction Computational Sciences" and "Numerical Linear Algebra" in my Bachelors, I would not have been interested in Computational Sciences. I would not have found the MSc Computational Sciences program, as Computational Sciences fits my interests and skill sets better than any other program I could have taken. For Rik and Martijn have forever altered my career trajectory.

Thank you to Sarah Flickinger for showing me the research that she has been doing in the lab. She allowed me to really connect my research and models to real life, reminding me that what I am doing has real life use cases than just a purely theoretical or programming challenge.

And finally, thank you to all of my friends for keeping me sane and helping me through both of my programs.

Contents

Declaration of Authorship	i
Abstract	iii
Acknowledgements	v
Contents	vi
List of Figures	x
List of Tables	xiii
Abbreviations	xiv
1 Introduction	1
1.1 Thesis Overview	1
1.2 Biological Background	2
1.3 The Environment	2
1.3.1 Phage’s Role in the Environment	3
1.3.1.1 Phages and Controlling Bacterial Blooms	3
1.4 Phage Cocktails and Human Health	4
1.5 Industrial Usage	4
1.6 Modelling Phages in a Complex Community	4
1.7 Software Overview	5
2 Literature review	7
2.1 Methods of Modelling Phages and Bacteria	7
2.1.1 Generalized Lotka-Volterra Model	8
2.1.2 Generalized Consumer-Resource Model	8
2.1.3 Trait-Based Model	9
2.1.4 Agent-Based Models	9
2.2 Phage Biology	10
2.2.1 What Are Phages?	10
2.2.2 How Does the Phage Cycle Work?	11
2.2.2.1 Infection Stage	12

	Detection and Attachment	12
	Phage DNA Injection	12
2.2.2.2	Lysogenic Cycle	12
	Repression of Phage DNA Detection	12
	Phage DNA Integration Into Bacteria DNA	13
	Cellular Replication	13
	Phage Induction	13
2.2.2.3	Lytic Cycle	13
	Hijacking DNA Replication Process	13
	Assembly of Phage Parts	13
	Lysis of the Bacterial Cell	14
2.3	Bacterial Defense Against Phages	14
2.3.1	Mutations in Bacterial DNA (Genetic (Co-)Evolution)	14
2.3.2	Horizontally Transferring DNA	14
2.3.3	Phage Inactivation and Decoys	15
2.3.4	CRISPR-Cas Methods	15
2.3.5	Phenotype Resistance	15
2.3.6	Spatial Refuge/Biofilms	15
2.4	Phage Counter Defense Against Bacteria	16
2.4.1	Genetic Mutations	16
2.4.2	Viral Recombination	17
2.5	Phage Defense Against Phages	17
2.5.1	Altering Cell Structure	17
2.5.2	Protein Creation	17
2.6	Bacteria and Phages in the Lab	18
2.7	Software Mathematically Modelling Phages, Bacteria, and Resources . . .	20
2.7.1	Cocktail	20
2.7.2	PhageDyn	20
2.7.3	Cocktail and PhageDyn Limitations	20
2.8	Growth Curves Typically Seen in a Lab	21
3	Methods	24
3.1	Project Overview	24
3.1.1	Network Creation Tool	24
3.1.2	Simulation Framework	27
3.1.3	Visualization Dashboard	28
3.1.3.1	Editing Network and Parameter Values	28
	Initial Condition	28
	Vector Data	28
	Matrix Data	28
	Environment and settings	29
3.1.3.2	Visualization and Analysis	30
	Serial Transfer	30
	Parameter Analysis	31
	Initial Value Analysis	32
	Phase Portrait	33
	SOBOL Sensitivity Analysis	34

Ultimate Analysis	35
3.1.4 Custom Visualizations and Analyses	37
3.2 The Golding Model	37
3.2.1 The Golding Model	37
3.2.2 The Adapted Golding Model	38
3.3 Software Used and Packages	38
4 Experiments and Results	41
4.1 Graph Behavior	41
4.2 SOBOL Sensitivity Analysis Results	41
4.2.1 Final Value Results	43
4.2.1.1 Resources	43
4.2.1.2 Phages	43
4.2.1.3 Total Bacteria	43
4.2.2 Peak Value Results	43
4.2.2.1 Phages	43
4.2.2.2 Total Bacteria	44
4.2.3 Time of Peak Value Results	44
4.2.3.1 Phages	44
4.2.3.2 Total Bacteria	44
4.3 Initial Value Analysis Results	45
4.4 Phase Portrait	45
4.5 Plotting Parameter Change - $3 \times 2 \times 3$ Model	46
4.6 Phage, Bacteria, and Resource Survivability For a $20 \times 20 \times 10$ System . .	49
5 Discussion	51
5.1 Graph Behavior	51
5.2 A Good Curve	51
5.3 SOBOL Sensitivity	52
5.3.1 Final Value Analysis	52
5.3.1.1 Resources	52
5.3.1.2 Phages	52
5.3.1.3 Total Bacteria	53
5.3.2 Peak Value Analysis	53
5.3.2.1 Resources	53
5.3.2.2 Phages	53
5.3.2.3 Total Bacteria	54
5.3.3 Time of Peak Analysis	54
5.3.3.1 Resources	54
5.3.3.2 Phages	54
5.3.3.3 Total Bacteria	55
5.4 Initial Value Analysis	55
5.5 Phase Portrait	56
5.5.1 3D Plot	57
5.6 Plotting Parameter Change	57
6 Conclusion and future work	58

6.1	Conclusion	58
6.2	Future Work	58
6.2.1	Other Models	58
6.2.1.1	Spatial simulations	60
	PDE	60
	Discretization	60
7	Ethics and Data Management	61
7.1	Ethical Considerations	61
7.2	Data Management	61
7.3	Adherence to Codes and Principles	62
A	Appendix A: Equation Parameters	63
A.1	Simple/Advanced Golding Model Parameters	63
A.2	SOBOL Parameters	63
A.3	Linear Regression Parameters	63
B	Appendix B: Industrial and Real Life Applications of Phages	66
B.1	Controlling Foodborne Bacteria	67
B.1.1	Current Applications	67
B.2	Phage Therapy and Antibiotics	69
B.2.1	Current Applications: Bacterial Infection Control	69
B.3	Environmental Protection	70
B.3.1	Current Applications	71
C	Appendix C: Flowchart of User and System Interactions	73
D	Appendix D: ODE Model Implementation	75
E	Appendix E: Parameter Values Used	76
E.1	A Good Curve	76
E.2	A Good Curve 2	76
E.3	SOBOL Analysis	76
E.4	Complex Model	76
F	Appendix F: Extra Plots and Figures	79
F.1	SOBOL Analysis With Washin and Washout	79
F.1.1	Final Value Analysis	79
F.1.1.1	Resources	79
F.1.1.2	Phages	79
F.1.1.3	Total Bacteria	79
F.1.2	Peak Value and Time of peak	80
F.2	Why 95%?	80
F.3	Varying r and β In A $3 \times 2 \times 3$ System	82
	Bibliography	87

List of Figures

1.1	Life cycle of a phage, inside and outside a bacteria cell. Significant steps in the life cycle of a phage include the infection stage, integration, replication, and lysing process. Figure sourced from Campbell [2].	2
2.1	Different models and how the bacterial agents interact with itself, one another, resources and the environment. All figures sourced from van den Berg et al. [3]	10
2.2	Parts of a phage, a real life picture of phages infecting an <i>E. coli</i> bacterium, and an artist's impression of phages infecting a bacterium.	11
2.3	Bacteria lawn, the dots on the petri dish show no bacteria growth due to the presence of phages. Photo courtesy of S. Flickinger.	19
2.4	Example output from Cocktail and PhageDyn respectively. For PhageDyn, concentration of heterotrophic biomass in an aerobic plug flow across four situations. See Nilsson [4] and Krysiak-Baltyn et al. [5] for more information on parameter values and supplementary resources.	21
2.5	Growth population of a $1 \times 1 \times 1$ system. The log plot allows to see behavior happening at values approaching and to plot data on a logarithmic scale. The parameters used for this plot can be found in Table E.1.	23
3.1	This network topography along with a $1 \times 1 \times 1$ network will be used in the Methods and Experiments and Results sections. The parameter values for the networks can be found at Table E.1, Table E.4 and Table E.3 Each node represents a phage, bacteria, or resource, with arbitrary interactions occurring between them. Although not shown and used here, edges between the same agent types and self loops are allowed.	26
3.2	The tabs where the user can edit the various parameter values and control the simulation parameters	29
3.3	Serial Transfer	31
3.4	Parameter Analysis	32
3.5	The IVA settings and output.	33
3.6	Phase portrait settings and output.	33
3.7	SOBOL variance analysis settings and output.	36
3.8	The ultimate analysis setup tab.	36
4.1	SOBOL analyses for the final, peak, and time of peak value, without a washin and washout rate. The input value ranges to test each parameter used for this SOBOL test can be found in Table E.3, except washin and washout was set to 0.	44

4.2	Varying initial Uninfected Bacteria concentration, from 50 to 500, with 30 unique values tested over two different instances of "good" curves. Even with two "good" curves, even varying the default parameter values a tiny bit can have a large influence on how changing the initial bacteria concentration can have an influence on the dynamics of the system, changing the behavior of the peak time. The default values for Figure a) and b) can be found at Table E.1 and Table E.2.	46
4.3	Varying initial resources and initial phages and the resulting proliferation and fitted proliferation curve. Proliferation is defined as when the phage population reached at least 2 times the initial starting population. This simulation values used can be found in Table E.2, but with washout set to 0.02 instead of 0.	47
4.4	3D plot of phage proliferation, dependent on initial resource, uninfected bacteria, and phage population. Color scaling from white to red, color is dependent on the max phage population reached.	48
4.5	Varying r , β , and ω^o . All phage values set to 10 to show how the network connections and vector/matrix values affect phage growth. Selectively chosen sub-figures from Figure F.3, Figure F.4, and Figure F.5. Chosen parameter values can be found in Table E.4.	50
6.1	Exponential growth curve vs logistic growth	60
B.1	SalmoLyse [®] reduces Salmonella contamination on various food surfaces: Mean and standard error bars shown. Statistical analyses were carried out for each food group independently. Asterisks denote significant reduction from corresponding controls based on one-way ANOVA with Tukey's post-hoc tests for multiple corrections: ** denotes $p < 0.01$, while *** denotes $p < 0.001$ compared to the corresponding controls. There was significant reduction in Salmonella on all food surfaces with the addition of SalmoLyse [®] compared to the controls; the mean percent reductions from the control are noted in the boxes above treatment bars. CFU/g D colony forming units per gram. Each letter denotes a food group that was tested with SalmoLyse [®] and compared to a control: A= chicken; B= lettuce; C= tuna; D= cantaloupe; E= ground turkey. Plot sourced from Soffer et al. [6].	68
B.2	<i>Salmonella</i> count in a mixture of 5 <i>Salmonella</i> strains spot-inoculated (CFU/g) onto a) lettuce and b) sprouts after spraying with a mixture of bacteriophage (SalmoFresh [™]) relative to positive controls at 2, 10 and 25C and stored for 1, 24, 48 and 72 h. Plot sourced from Zhang et al. [7]	68
B.3	Cyanobacteria degradation cycle, main hazards of cyanobacteria bloom to water bodies, aquatic organisms, and the human body. (DO: dissolved oxygen; SD: water transparency; Cond: conductivity; N: nitrogen; P: phosphorus; MCs: microcystins). [8]	71
C.1	The flowchart of user and system interactions. Read from top to bottom.	74
E.1	The log plot allows to see behavior happening at values near 0 and to plot data on a logarithmic scale. The parameters used for this plot can be found in Table E.1.	77

F.1	SOBOL analyses for the final, peak, and time of peak value with a washin and washout rate. The data was saved from the dashboard and plotted using Matplotlib. The values used for this SOBOL test can be found in Table E.3. The data used in Figure F.1a was used for Figure F.1b and Figure F.1c.	81
F.2	Testing the 95% rule vs the 100% rule, where the time at the absolute peak is taken and plotted in the second plot. A comparison of phages and uninfected bacteria is shown. Verification of the graph shape between the 95% rule graph and a frequent time step with 100% rule can be seen between c) and e). The e value is changed, ranging from 0.05 to 0.25. . .	83
F.3	Washout $\omega^o = 0$	84
F.4	Washout $\omega^o = 0.02$	85
F.5	Washout $\omega^o = 0.05$	86

List of Tables

4.1	A table that compares how moving one individual parameter value up or down relative to Figure 2.5a changes the general shape of the curve. This table is not meant to be exhaustive, cover edge cases, or extreme cases, or cover every exact detail and change in the population graph, but just to give an idea of how a change in parameter influences the graph shape, such as the rate of resource depletion, maximum number of bacteria and phages, and change in peak time. Reference parameter values used to compare the produced curves are included in the parentheses, taken from Table E.1.	42
A.1	Golding model parameters with variables, names, and descriptions. Subscripts on parameters indicate relationships; for example, e_{br} is nonzero if there is an edge connecting bacteria b to resource r in the network, zero otherwise.	64
A.2	SOBOL parameter symbols, name, and description.	64
A.3	Variable symbol, name, and description used for the linear regression. . .	65
E.1	The parameter values used for Figure 2.5.	76
E.2	Another set of "good" curves. The linear and logarithmic plot of this data can be seen in Figure E.1	77
E.3	The parameter values used for the SOBOL sensitivity analysis in Figure F.1, ?? and Figure 4.1.	78
E.4	The parameter values used for the $3 \times 2 \times 3$ network model rounded to 5 decimal points. If there is no edge between agents, then in the matrix representation of the parameter, NaN , short for Not a Number, is stored in the matrix data.	78

Abbreviations

DDE	Delay Differential Equation
DNA	DeoxyriboNucleic Acid
GUI	Graphical User Interface
IC	Initial Condition
IVA	Initial Value Analysis
NAN	Not A Number
OD	Optical Density
ODE	Ordinary Differential Equation
PA	Parameter Analysis
PDE	Partial Differential Equation
RNA	RiboNucleic Acid
ST	Serial Transfer
UA	Ultimate Analysis
UvA	Universitiet van Amsterdam

Chapter 1

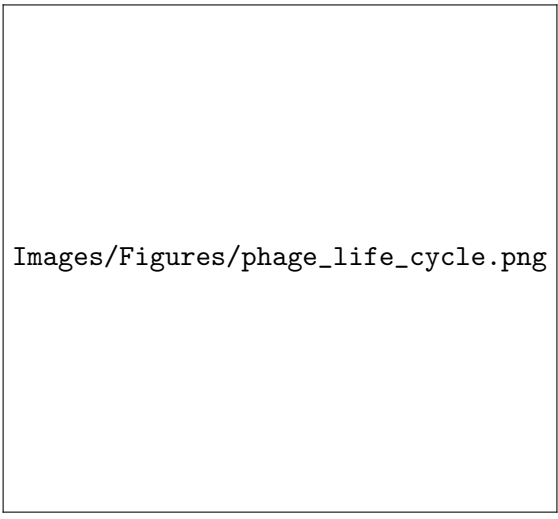
Introduction

Phages are small viruses on the order of 27-190nm that infect and lyse (kill) specific bacteria, acting as nature's natural anti-microbial defense. Researchers are attempting to determine how phages can be used in various medical and industrial applications to control bacterial growth. However, researchers need to know how the interactions between phages and bacteria work in order to implement a robust method to control bacterial growth.

1.1 Thesis Overview

This thesis covers multiple topics to ultimately answer how phages and bacteria interactions can be mathematically modelled. First, there is a (biological) introduction to phages and bacteria. This introduction covers how phages work and infect bacteria, how bacteria defend against phages, how phages defeat bacterial defenses, and how phages defend against other phages. There is also an introduction to different modelling techniques such as spatial vs non-spatial models and ODEs vs DDEs. This thesis briefly covers software that models phages, resources, bacteria, and their limitations.

This thesis presents software I developed to support the research, demonstrating its capabilities using a representative model of phage-bacteria-resource interactions. The section also provides an overview of its usage, including example outputs from demonstration runs. Finally, the results generated by the software will be thoroughly analyzed and discussed.



Images/Figures/phage_life_cycle.png

Figure 1.1: Life cycle of a phage, inside and outside a bacteria cell. Significant steps in the life cycle of a phage include the infection stage, integration, replication, and lysing process. Figure sourced from Campbell [2].

1.2 Biological Background

Phages are small viruses on the order of 27-190nm (the average size of marine phages are 54nm) that infect and lyse (kill) specific bacteria. Phages are so small, that it takes 55 million phages to cover the period at the end of this sentence [9]. The phage cycle process starts with a phage coming into contact with a bacterium. Once it has identified an injection site, the phage can inject a strain of DNA into the bacteria. The DNA strand has two options: it can either merge into the bacterial DNA, allowing the phage's DNA strand to replicate alongside the bacteria as they reproduce. This process defines the Lysogenic cycle. After a set amount of time, the DNA of the phage can unmerge and hijack the DNA replicating mechanism, creating multiple copies of itself, using the transcription, translation, and replication process to create multiple copies of itself. The phages begin to self-assemble inside the bacteria until the bacteria is full of phages and explodes, the lysis stage, releasing the phages into the environment, ready to repeat the process again.

This process can be visualized in Figure 1.1.

1.3 The Environment

In an ecosystem like the ocean, the gut, or in soil, there are thousands of different microbes all interacting with one another or the surrounding environment. The interactions are complex, with many factors affecting the growth of bacteria, phages, plants, animals, and more.

The interactions between agents in the environment are often synergistic. When an animal dies, bacteria start to digest and decompose the animal into simpler chemicals like carbon and nitrogen that plants can use to grow, which is then eaten by other animals. External factors, such as flooding, droughts, chemical spills, or introduction of new agents have a massive impact on the ecosystem. These events can add or remove resources from the system, change environmental parameters such as the surrounding temperature, introduce competition, or create an imbalance in the population by killing agents. These effects have a larger effect on the ecosystem and food chain as a whole as bacteria are one of the fundamental foundations for resource recycling.

1.3.1 Phage's Role in the Environment

Phages play a large role in the ecosystem. As bacteria die, for example through lysis, they release resources into the environment for other bacteria and plants to use. This turns over resources like nitrogen and carbon for other sources to use. Phages also help mediate horizontal gene transfer, disperse pathogenic diseases, and spread antibiotic resistance [10]. Phages directly alter bacteria population diversity and population fitness by introducing new ways for bacteria to mutate [11]. There are about 10^6 bacteria cells/ml and 10^7 phages/ml of marine water. About 5% of any bacteria are currently infected and about 15% of daily bacterial death can be attributed to phages [12].

Phage populations depend on growth by infection and death by degrading. UV is a large factor of killing marine phages, causing up to a 5% reduction in phage infectivity per hour [12].

1.3.1.1 Phages and Controlling Bacterial Blooms

Phages could potentially be used to control *Cyanobacteria* (blue-green algae) blooms in the environment [13]. *Cyanobacteria* cause damage to aquatic life by consuming resources and oxygen, starving aquatic life and negatively affect human health. There is hope that phages can be used to biologically control water quality in waste water treatment plants and in the environment without the use of harsh chemical processes what would otherwise pose environmental and health hazards [5, 14]. More information about controlling *Cyanobacteria* can be read in Environmental Protection.

1.4 Phage Cocktails and Human Health

There is particular interest in phage applications in human and animal health, called phage cocktail therapy, due to phage cocktails not exhibiting side effects. Phage cocktails are a medicine that sick patients with bacterial diseases, such as *Escherichia coli* can use. A patient can swallow a pill filled with a range of different phages that target *E. coli*. The phages will target the specific *E. coli* bacteria, but it will not affect the other bacteria found in the gut of the human body and will not have any side effects on the body. There are about 100 trillion microbes across 5,000 different types of bacteria strains in the human gut. Antibiotics disrupt the intricate ecosystem of the gut microbiome, acting as a scorched-earth mechanism. Phages on the other hand specifically target a specific bacterial strain, acting as a sniper, with minimal to no effects to other bacterial strains, while antibiotics act as a bomb. A challenge that antibiotics face is that antibiotics create antibiotic resistant bacteria, making the antibiotic less effective in the future [15, 16]. There is however hope that phage resistant bacteria become more susceptible to antibiotics due to changes in the cell structure [17, 18]. Phage Therapy and Antibiotics in Appendix B: Industrial and Real Life Applications of Phages goes more in depth on how phages can be used in a healthcare setting.

1.5 Industrial Usage

Phages have many uses in an industrial setting. Similarly, phage therapies can be used as a preventative method, by preventing the spread of common bacteria in livestock by dosing the animal feed with the phage pills. Farmers often raise livestock in tight spaces with a lack of sanitation facilities, increasing the risk of a disease spreading.

Phages can be used to control the growth of bacteria like *Salmonella* while producing food in a factory [6, 19]. Controlling Foodborne Bacteria in Appendix B: Industrial and Real Life Applications of Phages goes into more detail about using phages to control foodborne bacteria.

1.6 Modelling Phages in a Complex Community

Not much is known about phages in large and complex communities between other phages, bacteria, resources, and the environment. There have been previous attempts to model the complex dynamics of the populations between phages, bacteria, and resources, with the environment using Ordinary Differential Equations (ODE) and Delay

Differential Equations (DDE). Not every interaction in the complex community can be identified, and if an interaction has been identified, the associated parameter values are unknown and need to be experimentally derived. Collecting interaction parameter values is an expensive and laborious task, as the data has to be experimentally collected.

There are two main ways to model phage-bacteria dynamics: spatially and non-spatially. In a spatial model phages and bacteria can move through space and interact with their neighbors. Partial differential equations (PDE) and cellular agent-based models (ABM) have been used to model spatial interactions. Spatial models require special considerations, such as proximity to other agents. This creates areas of interaction and interest where agents are located, and areas of no interactions where there are no interactions. Spatial models lead to more computationally complex models, but can result in more interesting and biologically realistic results.

Whereas in non-spatial models such as ODEs and DDEs, the bacteria and phages are assumed to be in a well-mixed solution and no distinctions are made in regard to neighbors or distances to other agents. Interactions are simplified to a probabilistic approach, where a percentage p of agents interact with one another at time step t . Non non-spatial models are easier to develop, understand, and are more effective in modeling large populations, at the cost of losing spatial information.

For this thesis, the focus will be modelling resource, phage, and bacteria interactions using an ODE model. A phage-bacteria-resource system is described as an $p \times b \times r$ system, meaning p phages, b bacteria, Current modelling methods have mainly stayed with $1 \times 1 \times 1$ models, meaning 1 phage, 1 bacteria, and 1 resource. This thesis aims to develop a simulation framework that can model any $p \times b \times r$ ODE system, where each agent can contain states (called hidden agents) that they can move to and from.

1.7 Software Overview

The project is divided into three logical parts, with an optional fourth part. The first section is to create the network interaction. Here the user of the software can define the number of resources, phages, and bacteria, who interacts with who, and the strength and type of interactions. See Network Creation Tool for further information. In Simulation Framework, the user uploads the network model and parameters and as output receives the time data and population data as an array. Visualization Dashboard allows the user to interact with Network Creation Tool and Simulation Framework with a dashboard. The user can graphically edit the attribute values of the edges and nodes of the network,

and the user can run more advanced visualizations, for example by changing a parameter value and seeing how that affects the population count. There are a few plots included out of the box that the user can test. The plots offered in part 3 offer interactivity like hiding and showing lines and dots, zooming in and out, and hovering over the lines and dots to show more details of the data.

Finally, the user can optionally run multiple simulations and download the data to their disk to create their own custom visualizations using Custom Visualizations and Analyses. The visualizations created in Visualization Dashboard can theoretically be recreated in Custom Visualizations and Analyses. The user can choose the same parameter values used for a specific plot in Visualization Dashboard, run the simulation (under the Ultimate Analysis section), download the data, and reimplement the graphs.

The user can use the tool themselves by importing the Python classes in their own code and initializing the classes and passing the appropriate data.

Chapter 2

Literature review

2.1 Methods of Modelling Phages and Bacteria

There are numerous ways to model the interactions between phages and bacteria. Models can be built at a molecular level, where the model simulates the mechanical and chemical behavior of a phage as it interacts with the surface of a bacterium using computational chemistry and physics methods. On the other end of the spectrum, populations of phages, bacteria, and resources can be modeled using Ordinary Differential Equations (ODEs) or Delay Differential Equations (DDEs). DDEs are similar to ODEs, except where when ODEs are calculating the values of the equations at time t using time $t - 1$, DDEs can, but don't have to, use the value of the equation at time $t - \tau$, where $1 \leq \tau \leq t$. DDEs are a generalized version of ODEs and are significantly harder to analyze and find stability conditions than ODEs due to the dependence on the past [20].

One way to introduce a delay to populations is to force populations to go through stages, causing a delay in other events. For example, in the paper Geng et al. [21], infected bacteria go through M stages of infection, before lysing. The more stages there are, the longer the delay in seeing a rise in phage population. By decreasing τ (the latent period) in the model proposed by Geng et al. [21] (see Section 3.2), the throughput of bacteria going from stage i to stage $i + 1$ of infection increases, thus seeing a larger rise in phage population.

Each type of model has its pros and cons. With the molecular level model, the model is more complex and needs significantly more startup time, simulation time, and is much more complex. However, more information can be gained from the simulations and can guide research in creating phages for a certain type of bacteria. The ODE method is simpler to understand and easier to set up, but it can only capture large population

dynamics. Certain assumptions about the community interactions also have to be made, such as the constant washout of the bacteria. Each model can be further developed, for example by adding temperature and pH dependence, bacteria releasing nutrients, or if the bacteria concentration is above a certain threshold, the infection rate is lowered to model phages struggling to diffuse through a biofilm.

2.1.1 Generalized Lotka-Volterra Model

The Lotka-Volterra model, a first-order non-linear differential model, captures the dynamics between predators and prey. Any population can be modelled as such:

$$\frac{dB_i}{dt} = B_i \left(\left(r_i + \sum_j^N \alpha_{ij} B_j \right) - m_i \right)$$

where r_i is reproduction rate, α_{ij} is the devour rate of B_i on B_j . If α_{ij} is negative, then B_i has a negative effect on B_j , otherwise B_i has a positive effect on B_j . m_i is the removal rate of B_i . The interactions can be seen in Figure 2.1a

2.1.2 Generalized Consumer-Resource Model

The generalized Consumer-Resource Model models the growth of a population and resource dynamics between a population of bacteria B_i and a resource R_i .

$$\frac{dB_i}{dt} = r_i B_i \left(\sum_{\alpha} \Delta w_{i\alpha} C_{i\alpha} R_{\alpha} \right) - m_i B_i \quad (2.1)$$

$$\frac{dR_{\beta}}{dt} = - \sum_i C_{i\beta} R_{\beta} B_i + \sum_{\alpha, i} D_{\beta\alpha}^i C_{i\alpha} R_{\beta} B_i \quad (2.2)$$

$$\Delta w_{i\alpha} = \sum_{\beta} D_{\beta\alpha}^i w_{\beta}$$

Equation (2.1) describes the growth of population B_i and Equation (2.2) describes the resource dynamics and metabolism of resource R_{β} . Resource R_{α} can become resource R_{β} at rate $R_{\beta\alpha}^i$. Bacteria B_i reproduces at rate r_i dependent on the concentration of resources $\sum_{\alpha} C_{i\alpha}$. Bacteria die out at rate m_i . For a visual, see Figure 2.1b

2.1.3 Trait-Based Model

The Trait-Based Model is a model that takes into account external factors such as the temperature or pH of the system and can be modeled as follows.

$$\begin{aligned}\frac{dB_i}{dt} &= (r_i - m_i) B_i \\ r_i &= \frac{r_{i\alpha}^{max} R_\alpha}{R_\alpha + K_{i\alpha}} e^{S_i(T - T_{ref_i})}\end{aligned}$$

where r_i is influenced by the environment impact factor. S_i is the sensitivity to B_i to factor T , and with trade off if $r_i^{max} > \text{mean } r^{max}$ then $S_i > \text{mean } S$. The larger S_i is, and the larger the difference T is from T_{ref_i} , the stronger the effect will have on the growth rate of r_i . r_i follows the Monod equation, with $r_{i\alpha}^{max}$ being the maximum growth rate of bacteria B_i , R_α is the resource concentration, and $K_{i\alpha}$ is the affinity constant. Figure 2.1c shows the agent interactions in detail.

2.1.4 Agent-Based Models

ABMs model the system through space and time. An $x \times y$ grid is created and split into smaller sub-cells containing resources and microbes. Each cell acts as its own tiny environment, where resources and microbes interact within the cell, but not with the neighboring cells. Resources diffuse through the system using a PDE solver for a Boundary Value Problem (BVP). Agents can move into neighboring grids with a probability p , where p can depend on any number of parameters such as resource density, microbe density, or stochastic chance.

ABMs are useful when simulating many individual elements interacting in a system. Chaotic or emergent behavior can arise from these interactions. Chaotic behavior refers to the irregular and unpredictable evolution of a system's behavior due to nonlinear equations, exhibiting sensitive dependence on the initial condition (IC) [22].

Emergent behavior is behavior that arises from the interactions of various agents in a system, that was not explicitly programmed into the system. The behavior can be beneficial, neutral, or harmful, but it can not be predicted until it arises, *if* it arises. Agents can have simple rules, but when interacting with other agents, behavior that hasn't been programmed can arise. Sometimes, people consider systems with emergent behaviors more complex than the sum of their parts.

$$\frac{\delta R_\alpha((x, y), t)}{\delta t} = \nabla [D(R_\alpha, (x, y)) \nabla R_\alpha((x, y), t)] \quad (2.3)$$

Equation (2.3) describes the diffusion of resource R_α through the matrix cells, dependent on the resource concentration R_α at cell location (x, y) . The rules for cellular agents follow Equation (2.4).

$$\frac{di}{dt} = r_i \left(\sum_{\alpha} \Delta w_{i\alpha} C_{i\alpha} R_{\alpha} \right) \quad (2.4)$$

, where i is a bacterial agent, where if $0 \leq \text{threshold} \leq \frac{di}{dt} \leq 1$, some threshold, $\frac{di}{dt}$ expands into the neighboring grid cell with probability p . Agent i consumes resources and converts them into new resource with Equation (2.5).

$$\frac{dR_{\beta}}{dt} = \sum_i C_{i\beta} R_{\beta} I + \sum_{\alpha, i} D_{\beta\alpha}^i C_{i\alpha} R_{\alpha} i \quad (2.5)$$

Figure 2.1d shows how the agents interact with other agents in their cell.

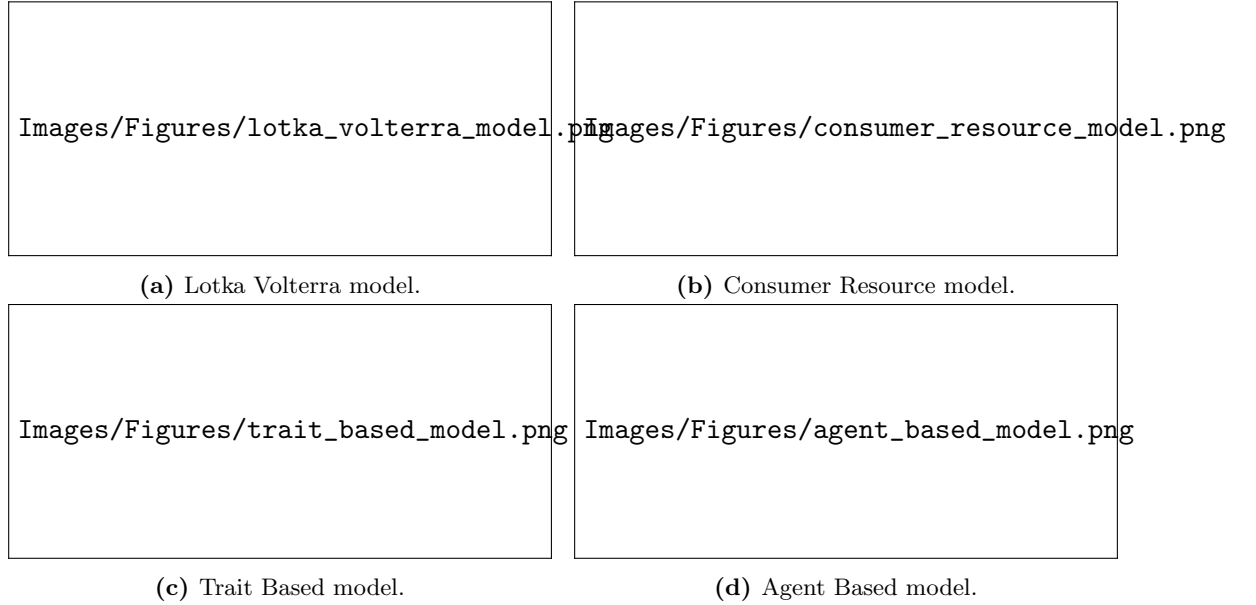


Figure 2.1: Different models and how the bacterial agents interact with itself, one another, resources and the environment. All figures sourced from van den Berg et al. [3]

2.2 Phage Biology

2.2.1 What Are Phages?

Phages are small bundles of proteins that contain viral DNA. Phages are made up of multiple parts built like LEGO to complete the task of infecting a bacterium. Figure 2.2a shows the body parts of a phage. The aim of the phage is to find a suitable bacterial host

and infect the host with viral DNA. The DNA alters the host's metabolic pathways to its benefit and hijacks the cellular replication process to create new copies of the phage. Eventually, the cell lyses, releasing the newly created phages into the environment to infect more bacteria.

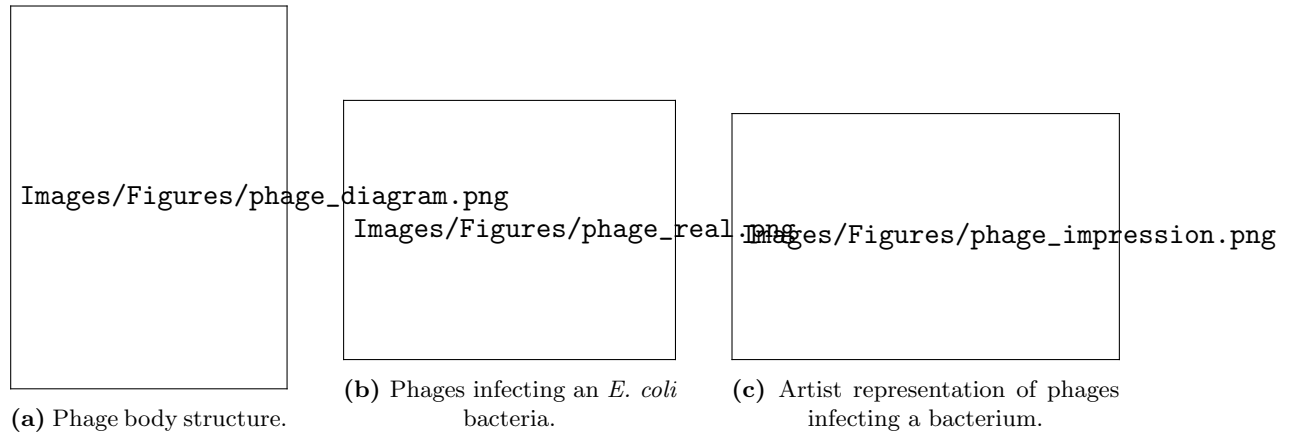


Figure 2.2: Parts of a phage, a real life picture of phages infecting an *E. coli* bacterium, and an artist's impression of phages infecting a bacterium.

2.2.2 How Does the Phage Cycle Work?

There are 3 main parts to the phage-bacteria host cycle, the infection stage, the lysogenic cycle, and the lytic cycle. In the infection stage, a phage floating through the environment detects and attaches to the surface of a bacteria cell. Once injected, the phage-cell pair can directly go into the lysogenic cycle or into the lytic cycle. Figure 1.1 shows a detailed overview of the phage cycle.

In the lysogenic cycle, the phage DNA injects integrates into the genome of the bacteria. As the bacteria undergoes cellular replication, the DNA of the phage will be copied with the cell. After a set amount of time, the phage DNA can cut itself from the genome and enters the lytic cycle.

In the lytic cycle, the phage hijacks the cellular process of the bacteria. The phage DNA hijacks the replication, transcription, and replication process of the cell, making more and more copies of phage. The phage parts build together to make a full part. Eventually the cell wall bursts releasing the phages into the environment ready to infect more bacteria.

2.2.2.1 Infection Stage

The infection stage is characterized as the searching for a bacterium, detection, and subsequent attachment and injection of DNA into the bacteria.

Detection and Attachment Phages float through the medium and by chance land on a bacteria. The phage detects the cell via phage receptor binding proteins located at the tip of the phage tail. Various inter-molecular forces such as hydrogen bonds help the phage detect and attach to the cell. The receptors are tuned to specific receptors found on the surface of the bacteria cell wall. Upon detection, conformational alterations in the phage's baseplate occur, causing changes in protein shapes, causing the sheath to contract and inject the viral DNA into the host. The successful binding and adsorption depends on the phage binding protein sensitivity, localization, and density of receptors. [23].

Phage DNA Injection The injection is triggered by the recognition between the phage's receptor-binding protein located at the tip of the tail and a specific receptor located on the surface of the bacteria. Once a suitable injection site has been identified, the phage injects the DNA into the cytoplasm of the cell. The specificity of recognition is directly related to the specificity of adsorption, which correlates to the structure of receptors located on the host's cell surface [23]. The injected DNA is called a plasmid, genetic structure usually in the shape of a circle that can replicate independently of chromosomes.

2.2.2.2 Lysogenic Cycle

The lysogenic cycle describes the process in which the viral DNA of the phage evades detection, integrates into the cell's DNA, replicates with the cell, and induces from the DNA. Prophages are phages that have integrated into the host's DNA.

Repression of Phage DNA Detection As phages are viruses, they need to evade viral detection methods such as Cyclic oligonucleotide-based anti-phage signalling systems (CBASS). CBASS triggers effector proteins that cause cell death, preventing phage replication and lysis [24]. Two big benefits of programmed cell death is that the cell death slows the growth of phages and the dead cells release resources into the environment, allowing other bacteria to recycle the resources and grow [25].

CRISPR-Cas is another method that bacteria can use to detect the presence of phage DNA. CRISPR-Cas is an adaptive immune system in bacteria that defends against phages by acquiring foreign DNA sequences (spacers) into its CRISPR array, transcribing them into CRISPR RNAs (crRNAs), and using these crRNAs with Cas proteins to identify and degrade foreign DNA [26].

Phage DNA Integration Into Bacteria DNA Phage DNA integrates into the bacterial genome as a prophage. This can alter host fitness by modifying metabolic pathways and cellular functions or increasing resistance to other phages, allowing the prophage to persist until conditions favor entry into the lytic cycle [25].

Cellular Replication The cell undergoes division multiple times, copying the prophage DNA into the cell copies. However prophages are still at risk of being discovered and excised by restriction enzymes [27].

Phage Induction Prophages induct (leave) from the bacteria DNA under specific conditions. The induction process starts with proteolytic cleavage and displacement of the phage repressor, which most of the time occurs upon activation of the SOS response following DNA damage [28]. Cell stressors such as DNA-damaging agents like UV light and antibiotics can jump-start the process to switch to the lytic cycle [23, 29].

2.2.2.3 Lytic Cycle

The lytic cycle describes the process in which the viral DNA hijacks the DNA replication process, assembles within the cell, and lyses the cell releasing the phages into the environment.

Hijacking DNA Replication Process The phage hijacks the cellular replication process to create the different proteins that make up the phage, like the legs, body, and head. Phenotypic reconfiguration of the host is frequently facilitated by auxiliary metabolic genes, which are genes initially sourced from host genomes but preserved and modified within viral genomes to channel energy and resources toward viral replication [25].

Assembly of Phage Parts Phage parts self-assemble by using various protein-protein and protein-nucleic interactions, along with other forms of interactions such as hydrogen bonding and hydrophobic/philic interactions [30].

Lysis of the Bacterial Cell Phages produce holin proteins that trigger and degrade the cell wall, releasing the phages and internally stored resources into the environment. Holins accumulate in the membrane until a specific time preprogrammed in the protein tells it to destroy the cell wall. The protein faces intense evolutionary pressure to control the length of the lytic cycle and ensure lysis at the optimal time [31].

2.3 Bacterial Defense Against Phages

There is a constant battle between phages and bacteria. The bacteria don't want to be killed by the phages, so they adapt defenses such as thickening of the cell wall, or once the viral DNA has integrated with the bacteria's DNA, the bacteria will cut the viral DNA out of their DNA using CRISPR and restriction enzymes [32].

2.3.1 Mutations in Bacterial DNA (Genetic (Co-)Evolution)

As bacteria cells grow and divide, random point mutations can occur in the DNA. These mutations can affect phage defenses, like thickening the cell wall or removing a receptor, making it harder for the phages to detect and infect the cell. Mutations can be partially effective if full effectiveness requires multiple steps to achieve. Mutations can fail or the mutation brings a cost to the bacteria cell by losing receptors on the cell wall [33].

2.3.2 Horizontally Transferring DNA

Bacteria can horizontally transfer DNA to other bacteria on contact. A donor cell can donate DNA fragments using a mechanism called the F-factor or plasmid with a pilus. The pilus acts as a tunnel between the donor cell and the recipient cell so that DNA can be transferred from the donor cell to the receiver cell. This method of sharing DNA can also have the unintended side effect where one bacteria will directly infect another bacteria by transferring phage DNA.

A phage can accidentally collect a piece of the host's DNA instead of its own DNA during assembly. The phage with the now dead hosts DNA can infect the next bacteria, injecting the new bacterium with the dead cell's DNA, horizontally transferring the DNA [34, 35].

2.3.3 Phage Inactivation and Decoys

Bacteria can further protect themselves by producing decoys that the phage will attach to instead of themselves. Freshly lysed bacteria may still have biomarkers that attract phages, leading phages to attach to non-viable cells where successful infection cannot occur. Bacteria can also produce proteolytic enzymes that will damage the proteins found in a phage [36]. Some bacteria can produce outer membrane vesicles that phages can absorb to, and later detach and float away with the phage [37]. It is suspected that the impact of these vesicles acting as a sink is minor [38].

2.3.4 CRISPR-Cas Methods

CRISPR is a gene editing tool that cells can use to cut out specified/unwanted parts of a DNA strand. Researchers are commonly using CRISPR to genetically engineer plants and animals to have specific features. Strands of DNA can be selectively added or removed from a DNA strand to achieve a better, more desired DNA strand. CRISPR defenses in the bacteria can detect the unwanted phage DNA and remove the DNA.

2.3.5 Phenotype Resistance

Although mutations can occur in bacterial DNA, not every mutation results in a distinct phenotypic change. However, there is still a chance that a mutation can change the phenotype representation. A mutation can cause the cell wall to thicken, making it harder for a phage to infect the cell. The bacterium can decrease the number of receptors that a phage can detect, making it harder for the phage to detect the bacterium.

Gupta et al. [39] found that some *Bacteroides fragilis* bacteria were able to evade phage infection. The presence of combinatorial phenotypic states where differential expression of protective mechanisms created rare super-resistant cells capable of withstanding phage attack. By acting together, these heterogeneously expressed anti-phage defense mechanisms created a phenotypic landscape where distinct protective combinations enabled the survival and re-growth of bacteria expressing these phenotypes without acquiring additional mutations.

2.3.6 Spatial Refuge/Biofilms

Usually bacteria and phages coexist in well mixed environments such as the ocean, however some environments offer natural structures for bacteria to hide behind. These

structures can range from physical structure, like sediment in water to biochemical structures like biofilms, where the phages can't diffuse through the biofilm. In large enough quantities, bacteria and other microbial communities create biofilms, a layer of mucus containing various microbes. The thick mucus, microbes, and other spatial effects help protect the bacteria in the biofilm from external phages by making it hard for the phages to penetrate and diffuse through the mucus [40]. In the case of a lab experiment on an agar plate, bacteria protect one another by making it harder for the phages to diffuse through the system [41].

Phage movement is passive, relying on diffusion through the environment or via pressure and temperature gradients [42]. Phages exhibit Brownian motion, the seemingly random movement of small particles throughout a medium due to other microscopic particles interacting and bouncing off of one another [43]. Unlike phages, bacteria possess motility, allowing them to actively move through their environment and escape nearby phages, increasing their chance of survival.

2.4 Phage Counter Defense Against Bacteria

With some of the defenses that bacteria have developed, phages are always mutating to counter their defenses. If phages don't adapt to the ever-changing bacterial defenses, the phages will die out due to their inability to infect and multiply. It essentially becomes a race to the bottom, seeing who can out-adapt the other.

If the phages out-adapt the bacteria too much, the bacteria die out, then eventually the phages degrade and die due to not having any bacteria left to infect. If bacteria out-adapt the phages, that is initially no problem for the bacteria because they don't need the phages to survive, and can keep on growing, limited only by the available space and resources. However, phages help transfer and turn over nutrients for the bacteria, as well as help transfer DNA between hosts, ensuring that the bacteria are genetically diverse. A delicate balance needs to be achieved so that both the bacteria and the phages can coexist.

2.4.1 Genetic Mutations

Mutations in viral DNA will affect how the phage body parts are designed and built. These mutations will affect external phage behavior such as how it detects a bacterium, as well as internal behavior such as evading detection and integrating with the cell's DNA. The changes will lead to changes in overall phage fitness, ie the ability for the phage to infect, replicate, and lyse bacteria.

2.4.2 Viral Recombination

Multiple phages can infect a cell and replicate itself using the cells internal replication process. Each phage has its own building blocks. When the phages are building copies of themselves, they could accidentally use the body parts of other phages [30]. The primary method for proteins to bond with other proteins and molecules is via hydrogen bonds. These attractive forces hold proteins and other molecules in defined positions, and a change in molecule shape will change the bonds, which will force the other molecule to undergo changes in shape. If the proteins that build the subparts of each phage have similar chemical properties, they can be swapped between phages. This allows for biological diversity to spread throughout a phage population. Each phage body part can have unique characteristics such as better attachment rate, larger DNA storage capsule, or better probability of injection.

Coexistence between phages and bacteria via genetic co-evolution seems unlikely due to trade-offs imposed by the new mutations [44].

2.5 Phage Defense Against Phages

Some phages can employ defenses against other phages from infecting the bacterial cell ensuring the hosts resources are all for itself. The act of preventing a secondary infection from a similar or closely related phage is called superinfection exclusion (SIE) [45]. There are various methods of preventing further infections that are listed below.

2.5.1 Altering Cell Structure

The prophage can alter the surface receptors of the bacteria, making it harder for other phages to detect the bacteria, reducing the chance of attachment and injection by other phages [46]. The prophage can hijack the internal metabolic pathway and cellular functions, affecting the genes that are expressed and transcribed to proteins.

2.5.2 Protein Creation

Other phages like the T4 phage can create proteins like the Spackle protein. The Spackle protein inhibits the lysozyme activity used in the process of DNA injection by other phages [46, 47]. Some prophages can encode proteins that will interfere with the replication process of other phages. For example, the SieA protein encoded by phage P22 blocks infection from other phages [48].

Tail Assembly Blocker (TAB) is an anti-phage defense mechanism encoded by a *Pseudomonas aeruginosa* prophage. While TAB permits the invading phage to replicate its genome, it inhibits the assembly of the phage tail, thereby preventing the production of infectious virions. The prophage that encodes TAB is not affected by this inhibition, as it also expresses a protein that neutralizes TAB's blocking activity. Although the host cell still undergoes lysis, no infectious phages are released.

2.6 Bacteria and Phages in the Lab

Researchers around the world are running lab experiments to gain further knowledge of the interactions between phages and bacteria. The aim is to better understand how phages work and interact with bacteria at a molecular, host, and population level.

A researcher might run the experiment in a liquid medium containing water, carbon and nitrogen sources, and other chemicals such as anti-foaming or pH control chemicals. This liquid medium, often referred to as broth, allows for the cultivation of bacteria in a well-mixed environment, enabling researchers to monitor bacterial growth and phage infection dynamics over time. By adjusting parameters such as resource concentration, temperature, agitation speed, and pH, researchers can simulate different environmental conditions and observe their effects on phage-bacteria interactions. Samples can be taken at various time points to measure bacterial density, phage titer, and resource concentration, providing quantitative data for model validation and hypothesis testing. If measured frequently enough, the researcher can get an ODE-like curve out, where each datapoint represents the population level at that time. Researchers create a mathematical ODE interpretation of the curve and run curve fitting algorithms to find the ODE model parameters. The tuned ODE parameter values tell the researcher the reaction rate speeds, the burst size of the cell, and cell latent period [1, 21]. Commonly used setups include chemostats and batch cultures. Chemostats allow for continuous addition of resources and removal of waste, maintaining steady-state conditions ideal for studying long-term dynamics.

Petri dishes are another commonly used way to grow bacterial colonies. Agar, a jelly-like substance derived from seaweed, is commonly used as a solid growth medium in petri dishes. Agar provides a stable surface for bacteria to grow on and form visible colonies. Researchers can tailor the nutrients and resources in the medium to support the growth of specific bacterial strains or to test the effects of different environmental conditions. When phages are introduced, clear zones called plaques appear where phages have infected and lysed the bacteria, allowing for quantification and observation of phage activity. As a cell lyses, it releases phages into the surrounding. The phages can diffuse

through the system, infecting neighboring cells. Phage infection creates clear plaques (2-3 mm) where bacteria are absent. See Figure 2.3 for an example.

Bacteria density in clear liquid mediums can be measured optically using light. As the bacteria grow and die, the solution will get more cloudy. By shining a light through a vial with bacteria growth, the change in light refraction and intensity can be measured. A researcher might also be interested in using a mass spectrometer to measure the density of phages and resources at specific time points.

With petri dishes, it is harder to measure the bacterial growth. Bacteria are mixed with phages in a heated liquid agar solution, and poured onto a petri dish. It might be possible to wash the bacteria off into a container to measure the optical density (OD), but the results are not always consistent. Measuring OD is inaccurate and can only accurately measure up to an OD of 0.1. Even though using a special spectrophotometer allows consistent results, the results are dependent on the medium, the length of travel through the medium, bacteria size and density. The device and measurements need to be calibrated to ensure proper results. Changing methods to using $\frac{\text{cells}}{\text{ml}}$ instead of OD can be used to directly compare results across experiments, labs, and bacteria colonies [49].

A computer vision algorithm might be able to quantify the change in color on the petri dish, by comparing the photo of the bacterial lawn with a reference photo with no bacteria growth. The algorithm could alternatively calculate plaque sizes and determine phage concentration. The results are however sensitive to camera settings and external lighting changing the room brightness.



Figure 2.3: Bacteria lawn, the dots on the petri dish show no bacteria growth due to the presence of phages. Photo courtesy of S. Flickinger.

2.7 Software Mathematically Modelling Phages, Bacteria, and Resources

Some software programs modelling phage-bacteria-resource interactions already exists.

2.7.1 Cocktail

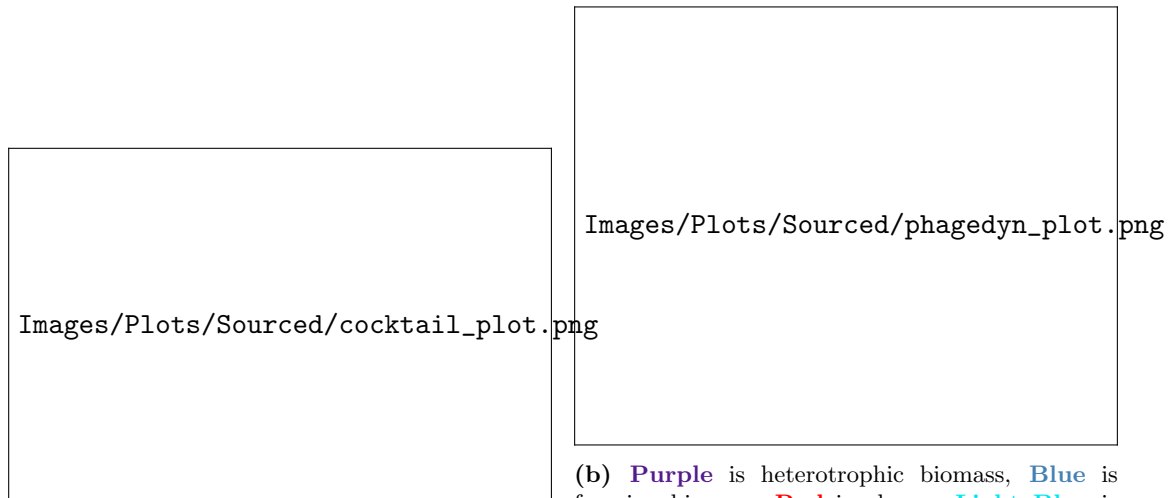
Nilsson [4] developed Cocktail to model phage-bacteria-resource kinetics in a chemostat. The model assumes there is one bacteria strain that can be infected by phage A and phage B, and by both phages at the same time, phage AB. The model models bacterial resistance to phage A, B, and AB. The user can control the parameter values such as resistance rate to A, B, and AB, resource concentration and outflow, and phage adsorption rate. The user can also control model settings, such as if the model is deterministic or stochastic, and the step size [4]. Four sample output plots are shown in Figure 2.4a.

2.7.2 PhageDyn

PhageDyn is a Java applet that models phage dynamics in multi-reactor industrial wastewater treatment plant models. PhageDyn interacts with existing GPS-X [50] files to incorporate phage dynamics into models of industrial wastewater treatment plants [5]. Krysiak-Baltyn et al. [5] developed PhageDyn to determine how phages can reduce foaming caused by bacteria in wastewater treatment plants, another real life application of phages [51]. PhageDyn does not simulate phage dynamics on its own but rather manipulates existing files in GPS-X in order to incorporate phage dynamics in wastewater treatment plant models. Figure 2.4b shows the output that PhageDyn provides.

2.7.3 Cocktail and PhageDyn Limitations

There are limitations to Cocktail and PhageDyn. Cocktail can model up to a $2 \times 1 \times 1$ system, and is designed to model a chemostat. Constant resources are being added into a chemostat, with the constant addition and removal of medium from the chemostat. Cocktail's model can not be easily adapted to other models. The ODE model accepts inputs from a hardcoded GUI frontend. So any changes to the frontend or to the ODE model will require changes to the ODE model and the frontend to accept the new inputs and outputs. The code for Cocktail is open source, so adding new buttons and changing the model should not pose a significant challenge, but still an undertaking.



(a) Figure A) *E. coli* infected with phage T4 in a chemostat exhibiting an oscillating growth behavior, following the model of Bohannan and Lenski [52]. Figure B) Oscillations of bacteria and phages can exist at higher titers, dependent on low resource concentration, following the model of Lenski [53]. Figure C) As the concentration of resources change, this results in increasing oscillations, but not going extinct. Figure D) A system modelling the interactions with phage A and B.

(b) **Purple** is heterotrophic biomass, **Blue** is foaming biomass, **Red** is phages, **Light Blue** is total suspended solids. Figure A) Biomass concentration immediately post phage dosing. Figure B) Biomass concentration with low phage concentration and maintain low concentration post spike in population count. Figure C) Biomass concentration when phages are extinct. Figure D) Biomass concentration with a less virulent and low adsorption rate phage, co-existence with biomass reached. A change in phage concentration shows a decrease in heterotrophic and foaming biomass [5].

Figure 2.4: Example output from Cocktail and PhageDyn respectively. For PhageDyn, concentration of heterotrophic biomass in an aerobic plug flow across four situations. See Nilsson [4] and Krysiak-Baltyn et al. [5] for more information on parameter values and supplementary resources.

PhageDyn works with GPS-X, a very niche wastewater treatment modelling software. PhageDyn is programmed for a very specific task with no flexibility in changing the model or inputs. PhageDyn assumes biomass, instead of individual bacteria populations. To the best of my ability, I could not find a copy of PhageDyn. When clicking on the link in the supplementary material of Krysiak-Baltyn et al. [5] to download a copy of the Java applet, the link returned a "URL Not Found" error.

2.8 Growth Curves Typically Seen in a Lab

When choosing parameter values it is important to choose parameter values that could realistically be found in real life systems and be replicated in the lab. Bacteria populations can double every 20-30 minutes, so if the growth rate is set to that it takes 1 day to double, the parameter choice is not good. There are various features that a researcher will be looking for in growth curve produced in a lab. A combination of these features results in a plot/graph/curve being called "good", while when those features are missing they are a "bad" graph.

There is a clear exponential rise in bacteria growth, and can expect to grow 40-100x in the span of a few hours. At a certain point in time, the bacteria population stop growing and start dying, almost as fast as they were growing. The shape should have a clear and pronounced growth, peak, and death.

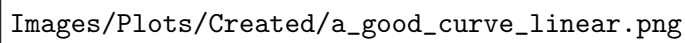
Phage populations also exhibit exponential growth, but with a delay in growth. The phage population will peak a few hours after the bacteria population reached its peak. If there is no phage death or removal, the phage population will eventually reach a plateau when every bacteria has died.

Figure 2.5a shows an example of a curve for a $1 \times 1 \times 1$ system that would typically be seen in a lab, and thus can be called "a good curve". Figure 2.5b is the same plot but with a logarithmic y-axis. Those specific plots can be classed as a "good curve" due to the plots exhibiting a clear growth, peak, and death cycle.

Once the resources reach 0, bacteria stop being created.

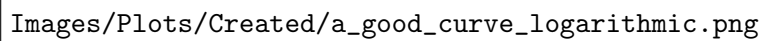
The uninfected and infected bacteria exhibit exponential growth, peaking at $t = 3.99$ with 1617 uninfected bacteria and at $t = 5.27$ with 3463 infected bacteria respectively. Resources start to deplete at $t = 4$, coinciding with the peak of the uninfected bacteria. The resource consumption rate starts to slow down at $t = 5$ as more bacteria are being killed than being created. This effect creates a decreasing sigmoid shape in the resource concentration curve, as the consumption of resources are proportional to the current bacterial population. The total bacteria population curve does not have as strong of a peak as the uninfected and infected curve, but the peak of 3805 bacteria at $t = 4.89$ is still clear.

The phages saw a significant increase in population count at around $t = 4$, coinciding with the peak in uninfected bacteria. There is a delay between the peak of bacteria at $t = 5$ and when the phage population reaches its effective max population at $t = 10$. The total bacteria population reached a peak of 3805 at $t = 4.89$, a 76.1x increase in population count from the initial 50 starting uninfected bacteria. The phage population reached a peak of 2584 phages at $t = 15$, a 258.4x increase in population count from its initial 10 phages.



Images/Plots/Created/a_good_curve_linear.png

(a) An example linear y-axis for a curve that researchers aim to get, can be called "a good curve".



Images/Plots/Created/a_good_curve_logarithmic.png

(b) The equivalent logarithmic y-axis plot for a curve that researchers aim to get, can be called "a good curve".

Figure 2.5: Growth population of a $1 \times 1 \times 1$ system. The log plot allows to see behavior happening at values approaching and to plot data on a logarithmic scale. The parameters used for this plot can be found in Table E.1.

Chapter 3

Methods

3.1 Project Overview

To help complete this Master thesis, I created various tools that would help create the final model outputs. The project is divided into four parts. The first part is the tool that a user can use to design and create the network of agent interactions. The second part is the simulation framework that handles the data and runs the ODE solving method. The third part is a dashboard that runs in the browser. The dashboard allows for a user to interact with the model, for example by changing parameter and environment values, and run some basic simulations and receive different plots as output. The final part allows the user to download the simulation data to create their own custom graphs and analyses.

A flowchart showing the user-system interactions can be seen in Appendix C: Flowchart of User and System Interactions.

3.1.1 Network Creation Tool

The network creation tool is the first step that a user needs to use, and it revolves around using a GUI tool built to create and edit the graph representation of the agent interaction. Numerous interactions occur between agents in a microbial environment. However, not every agent can and will interact with one another. Based on which agents interact with one another, a network topography representing the agent interactions and dynamics can be created.

Every node represents a unique agent, and each agent has their own intrinsic properties. The user can intuitively define agents, their interactions, environmental and model settings using the GUI tool. This tool allows users to quickly and intuitively define agents and their attributes, agent interactions and their attributes, environmental data, and model settings. An edge links two agents together if there is an arbitrary interaction occurring between the agents, with the properties exhibited in the interaction dependent on the interacting agents. Self interactions are allowed in the network. There is an environment node that is used to store global environmental data, such as the temperature and pH of the system. The settings node holds information such as simulation length, max time step, and the type of ODE solver to use. The tool provides functionalities for adding, editing, and visualizing nodes and edges, as well as importing and exporting the network structure.

Once the user is happy with the graph shape, they can export the network representation for use in Simulation Framework, Visualization Dashboard, and Custom Visualizations and Analyses. The most important part is that the user defines the shape and the attributes of the network, as that can't be edited in part 2 onwards. It is possible go back to the network creation tool and upload the graph to the tool to be able to edit the network representation.

The user can edit the values of the attributes in Visualization Dashboard, so the parameter values do not have to be perfect. As such, the user does not need to keep on using the GUI tool to edit parameter values.

Figure 3.1a shows the layout of the GUI tool. Figure 3.1c shows an example network that can be created. There are numerous buttons that can be used to edit the graph, for example adding or removing nodes and edges. By default, an environment node holding parameters such as pH and temperature is added. A settings node is added as well, holding settings data to be used for the solver, like the type of solver or simulation length. Manually adding nodes and edges can get tedious and repetitive for large graphs, so the user can add multiple nodes and edges at the same time. Nothing can interact with the environment and setting node, as they are used to hold data about the environment and network solver. The user can alter the default attribute name and value by importing the GUI tool class and overriding the method implementation implementing the default names and values. The user can self-decide which parameter values to give, and if and how the parameter values are randomized.

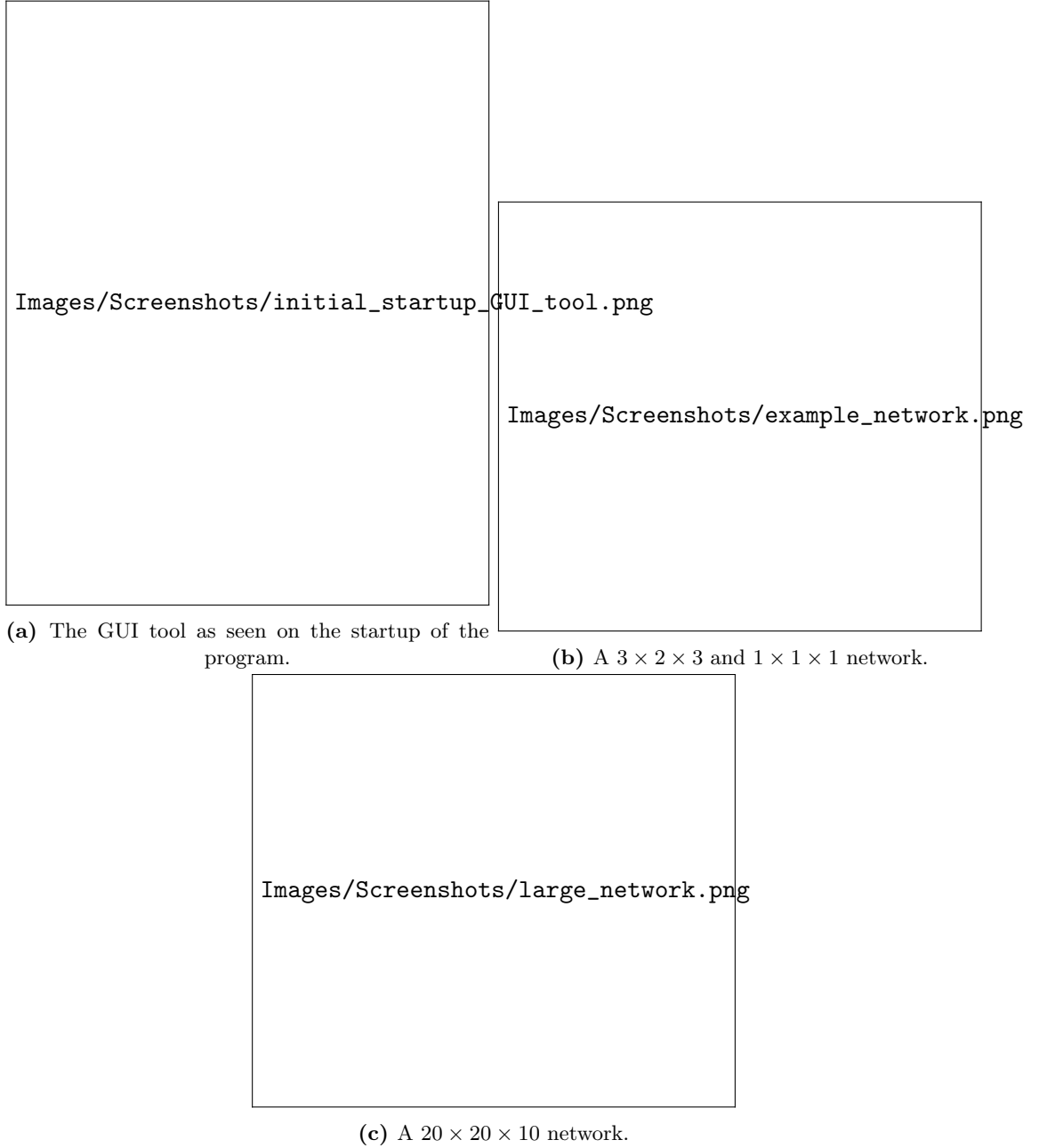


Figure 3.1: This network topography along with a $1 \times 1 \times 1$ network will be used in the Methods and Experiments and Results sections. The parameter values for the networks can be found at Table E.1, Table E.4 and Table E.3. Each node represents a phage, bacteria, or resource, with arbitrary interactions occurring between them. Although not shown and used here, edges between the same agent types and self loops are allowed.

3.1.2 Simulation Framework

The user provides an ODE model and the network topography as input to the framework. The simulation framework deals with handling the input, output, collecting and storing of the simulation input and output. The framework uses SciPy's [54] `solve_ivp()` numerical solver [55] to simulate the provided ODE equations and calculate the population levels through time. The user receives two outputs from the framework. The first output is an array of time values that the solver used to calculate the population count. The second output is an array containing the population count at each time step for every agent.

In order to facilitate more complex model behavior, "hidden" agents can be added to the simulation, where the hidden agents represent states that a "visible" agent can be in. Such an example would be the distinction between uninfected and infected bacteria. Each bacteria agent B_b would contain two hidden sub-agents, called sub-agent states, an uninfected state sub-agent U_b , and infected state sub-agent I_b . It is possible to further create sub-agents, by having a bacteria go through M stages of infection. So each infected agent would have sub-agent I_{b_k} where $1 \leq k \leq M$.

In the network model you would explicitly create a $3 \times 2 \times 3$ network, but when passing the network to the simulation framework, you would tell the framework to model the subagents. The user's ODE model has to correctly model each (hidden) agent and correctly handle the changes in states.

Even though the user might submit a $3 \times 2 \times 3$ model, if the user follows the uninfected and infected classification, where each bacterium goes through 4 stages, the ODE model and framework will explicitly be modelling 3 phages, 10 bacteria (2 uninfected + $2 \cdot 4 = 10$ infected bacteria), and 3 resources.

The user might also be interested in modelling a resource reservoir in a chemostat, where resources go from an external reservoir not accessible by the bacteria to the virtual chemostat ready to be consumed by the bacteria. 3 hidden resource agents would be added to the system, where the resources would model the transfer of resources from the reservoir to the simulation environment. The provided ODE model will have to correctly model and transfer the resources from $R_{r_{\text{reservoir}}}$ to $R_{r_{\text{chemostat}}}$, where $R_{r_{\text{reservoir}}}$ is inaccessible by the bacteria and $R_{r_{\text{chemostat}}}$ is accessible by the bacteria. It is then up to the user to determine how the resources are transferred, if the resources are added at constant intervals or continuously.

3.1.3 Visualization Dashboard

The third part involves analyzing and visualizing the simulation results on an interactive Dash Plotly [56] dashboard. The user can use a dashboard built using Plotly Dash to interact with the solver and network. The user can interact with the solver and network by changing parameter, environment, and setting values on the fly. This allows the user to quickly change parameter values and test different situations. The dashboard includes various starter plots that allow the user to test the model. As output, the dashboard will show interactive plots so that the user can analyze the system.

The dashboard allows the user to interact with the network, the model, and some prebuilt visualizations, and is built into three logical sections. The first section allows for the user to edit the network parameters and setting values on the fly to quickly iterate through different conditions and to fine-tune parameter selection without having to rebuild the network using the GUI tool. The second section allows for the user to see how the population count evolves over time for a given IC and parameter values, allowing to quickly test the network input. The final section allows for the user to run more advanced analyses on the network, for example, by changing multiple parameter values and visualizing the output.

3.1.3.1 Editing Network and Parameter Values

The editing network and parameter value contain five separate sections.

Initial Condition The IC settings panel (Figure 3.2a) allows for the user to edit the initial starting values of the agents. Each agent type has a table containing the initial population count. Extra hidden agents can be included. When a bacteria has been infected, the bacteria goes through multiple stages before lysing. Each bacteria agent starts out as uninfected, and once infected, the bacteria goes through 4 stages of infection before lysing as seen in Figure 3.2a.

Vector Data Data that can be represented as a vector, for example the data attributed to an agent type have their own section, Figure 3.2c.

Matrix Data Data that is stored as a matrix, the data stored on edges between agents, is stored in the matrix tab (Figure 3.2b).

Environment and settings The environment data and settings data also have their own tab, Figure 3.2d and Figure 3.2e respectively.



Figure 3.2: The tabs where the user can edit the various parameter values and control the simulation parameters

3.1.3.2 Visualization and Analysis

In the analysis section, the user can run different analysis methods to gain a greater understanding of the model. For simplicity, the visualizations only support a $1 \times 1 \times 1$ model, in order to make the analysis easier for the user, and to make it easier to analyze the visualization as the aim of the tool is to gain a deeper understanding of the interactions in a reduced complexity environment. These advanced visualizations were created with the mind of understanding a simple network. There are five different analysis and visualization methods, and one system where the user can run a large simulation on the whole network and receive an output file containing the raw simulation file data. The raw data is stored as a *parquet* file, a tabular-like data format, which when combined with Dask [57], allows for querying of the data similarly to Pandas. Parquet with Dask offers superior performance and data storage solutions that Pandas can't offer. Once queried, the user can create their own graphs and plots as they have access to the parameter values used and the raw simulation data.

Serial Transfer Serial transfer (ST) is a method employed by bacteriologist where after a set amount of time, the bacteriologist pipettes a specified amount of media (for example 10ml of liquid) containing bacteria and resources, possibly with phages, and transfers the old media into a solution containing new media. At this stage, the bacteriologist can introduce new agents, or re-introduce agents if the agent population or concentration has died out. However, usually only resources are added during the transfer process. An example would be an experiment starts with 50ml of solution. The experiment runs for 24 hours before 5ml is removed. Researchers can run various tests, such as using optical density measurements to assess bacterial density in the solution or employing a mass spectrometer to determine the concentration of the resources. The 5ml is then re-added to a new solution of 45ml containing fresh resources. The effect that this has is it creates a sort of artificial stable point. As the bacteria grow, they consume the resources found in the solution. However eventually the resources run out, and the bacteria die out due to a lack of resources. By introducing new resources at set time intervals, the bacteria can regrow and exhibit a semi-stationary behavior.

The implementation of ST is slightly different. A user can select a number which will divide the population count of the agents by that number (Figure 3.3a). Then the program takes the IC values defined for the resources the IC in Section 3.1.3.1 and adds those values to the resources respectively. By selecting a checkbox, the values as defined in the IC box for phages and bacteria in Section 3.1.3.1 can optionally be added as well. As an example, if at the end of a simulation, there are 120 resources, 5000 bacteria, and 1000 phages remaining and the chosen ST value is 15, then the resource, bacteria, and

phage values would be decreased to 8, 333.33, and 66.66 respectively. Then, if the IC for the resources, bacteria, and phages in Section 3.1.3.1 are 500, 80, and 10 respectively, and the checkbox is unchecked, the new population count will be 508, 333.33 and 66.66 respectively. If the checkbox is checked, the new population count will be 508, 413.33, and 76.66 respectively. These new values would be used as the new starting IC for a new simulation, and the run results will be appended to the previous run. As output, new graphs are created showing the runs appended to one another, with an example output shown in Figure 3.3b.

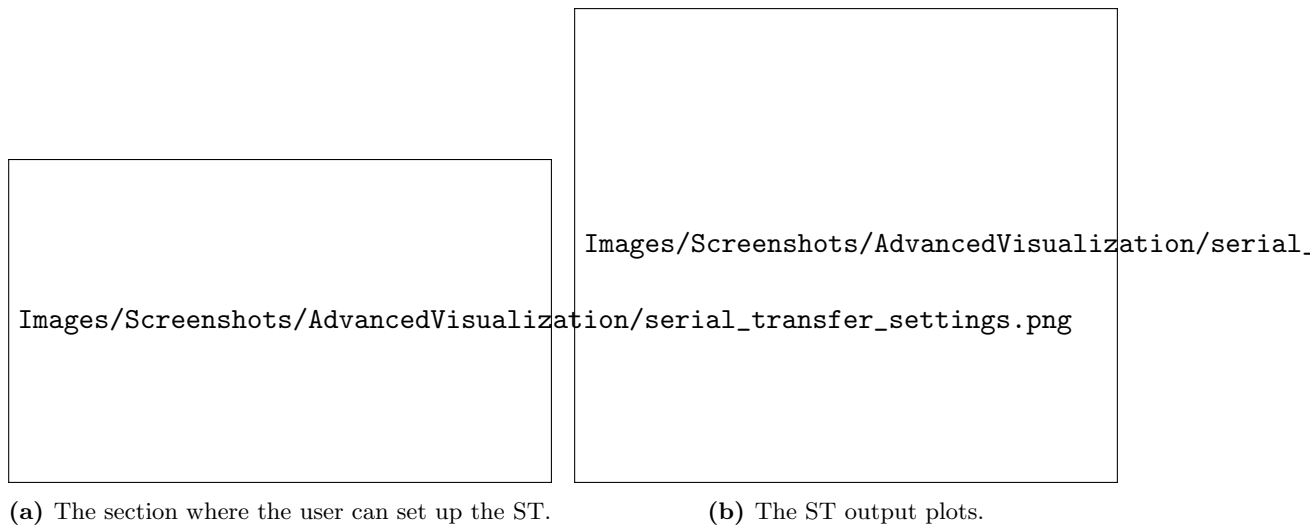


Figure 3.3: Serial Transfer

Parameter Analysis The parameter analysis (PA) settings tab as shown in Figure 3.4a allows the user to choose two parameters and individually run the model with the varying input values. The values that can be tested and changed include all IC values, vector and matrix data, and environmental data. As input, the user can select 2 parameters of choice. After the parameter name selection, the user can manually choose which parameter values they want to test or test a range of values equally spaced by selecting the number of values to test. Finally, the user can optionally run a ST, where the ST uses the settings found on the ST tab.

Figure 3.4b shows the heatmap that the user can expect, one heatmap for each agent type. Each heatmap cell represents the input of 2 unique parameter values, and shows the population count for that parameter run at the time shown in the slider. As the user slides the slider, the value inside the cell updates to correspond with the selected time. Note that the heatmap color range resets for each heatmap, so similar colors across heatmaps and across time will not correspond to the same values.

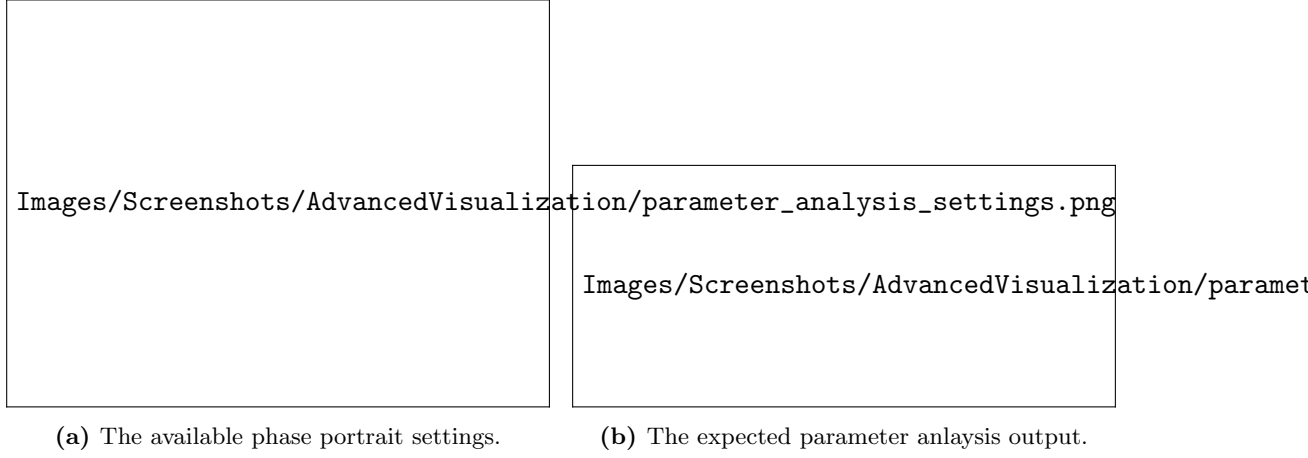


Figure 3.4: Parameter Analysis

Initial Value Analysis The initial value analysis (IVA) settings tab as shown in Figure 3.5a allows the user to choose a single parameter and vary the value of that parameter, visualizing how a change in parameter value affects the population count of the agents.

Figure 3.5b shows the plots that the user receives. For each agent type, there are three plots made. The left plot shows the population count through time, one line for each parameter value submitted. The middle plot takes each run and calculates the “percentage from the max value“ (default value of 0.95 \rightarrow 95%) reached of the peak. This value is considered the time of peak, and is used to fix some issues that can arise where the population plateaus or only keeps on rising. The initial value is plotted on the x-axis, with the time at which the max value is reached on the y-axis. Using the plotted data, a linear or log fit can be created. In Figure 1 of Mulla et al. [1], they vary the initial bacteria concentration and measure the time until bacterial collapse. The initial concentration and corresponding collapse time are plotted on logarithmic x and y axes, with a linear regression fitted to the log-transformed data. The observed logarithmic decrease suggests that the phage kinetics is adsorption-limited. Figure 4.2a replicates this graph.

The R^2 value, or coefficient of determination, is calculated as $R^2 = 1 - \frac{\sum_{i=1}^n (y_i - \hat{y}_i)^2}{\sum_{i=1}^n (y_i - \bar{y})^2}$ where y_i is the observed values, \hat{y}_i is the predicted values, and \bar{y} is the mean of the observed values.

Using the IVA tool can be useful for understanding how a change in parameter value affects the time at which the population count reaches a maximum. The slope, intercept and R^2 value is stored and saved in the third plot, a bar chart, with an editable name. For every re-run of the IVA, the slope, intercept and R^2 value is stored in the bar chart. When executed with multiple parameters, this enables comparison of high-level results

across various parameters and experimental conditions. The analysis can then be boiled down to the R^2 , slope, and intercept line to describe how the parameter value affects the peak value and time.

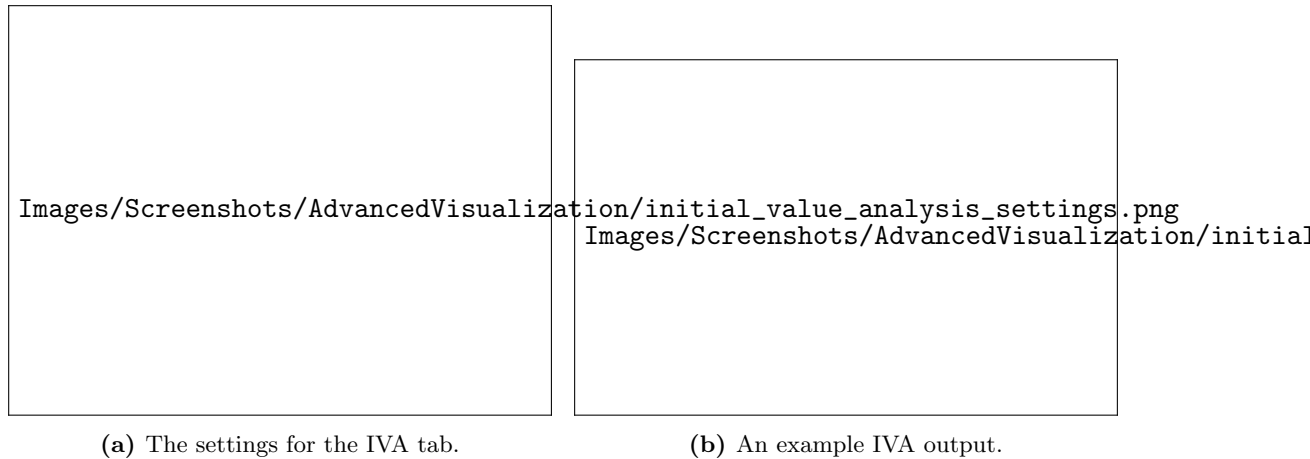


Figure 3.5: The IVA settings and output.

Phase Portrait The phase portrait plot allows the user to analyze how an agent population evolves with respect to the other agent population through time. Phase portraits indicate how one population increases while the other decreases, and vice versa. Steady states can be identified and classified as either stable, unstable, or as saddle points. It is also possible to visually identify attractor and repeller points by seeing where the population values trend towards. By comparing different starting points, it is possible to see if the system is chaotic or not. The setup for the phase portrait can be seen in Figure 3.6a, and a sample output can be seen in Figure 3.6b.

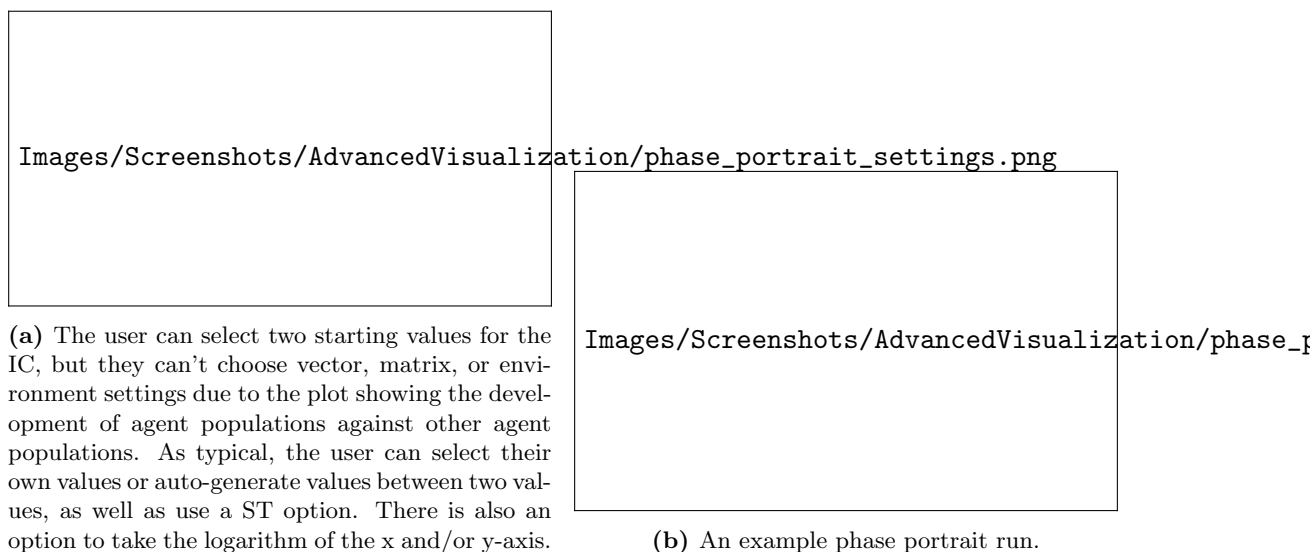


Figure 3.6: Phase portrait settings and output.

SOBOL Sensitivity Analysis It is important to understand how a change in parameter value affects the change in output of a model. Models will have parameters that are more important and have a larger effect on the model output than other parameters.

SOBOL analysis, a variance-based sensitivity analysis, is a method that allows a user to quantify how important an input parameter has on a measured aspect of the output by changing the input parameter values of the model and measuring the change in model output. SOBOL can only measure a single univariate model output, for example the final population value, smallest or largest value reached, the time at which the largest value was reached, or any other univariate output. SOBOL quantifies how much variance in the output can be attributed to a specific parameter and can measure the effect of global/total (ST), first ($S1$), and second order sensitivity ($S2$).

Global, also called total sensitivity, is the summation of all higher order interactions. First order Si , or local sensitivity, is the measurement of the effect that parameter i has on the variance of the output. Second order is the measurement of parameter i interacting with parameter j , and how the interaction attributes to the output variance. Etc for third order and higher. If $ST_i \gg S1_i$, then parameter i depends on higher order interactions with other parameters, while when $ST_i \approx S1_i$, then i doesn't interact much with and depend on other parameters. It should be stated that $ST_i \geq S1_i$ and that ST_i can be greater than 1, while $S1_i \leq 1$.

When a model is viewed as a black-box model, the model can be seen as a function $Y = f(X)$, where X is an input vector of d elements, and Y is a univariate model output. X is assumed to be independently and uniformly distributed within a hypercube $X_i \in [0, 1]$ for $i = 1, \dots, d$. The first order sensitivity measures the output variance of the main affect of parameter X_i . Measuring the effect of varying X_i averaged over other input parameters, and standardized to provide a fractional contribution to the overall output variance. The first order sensitivity is described as

$$S1_i = \frac{V_i}{Var(Y)}$$

where $V_i = Var_{X_i}(\mathbb{E}_{X_{\sim i}}[Y|X_i])$ and where $X_{\sim i}$ represents all the parameters that are not X_i . All parameters are summarized in Table A.2

The second order index measures the impact of input X_i interacting with X_j . For many inputs, this becomes unwieldy to analyze. The global sensitivity is used to analyze the global sensitivity without evaluating $2^d - 1$ indices, and measures the contribution to the output variance of X_i , including all variance due to X_i 's interaction with other variables.

$$S1_i = \frac{\mathbb{E}_{X_{\sim i}}[Var_{X_i}(Y|X_{\sim i})]}{Var(Y)} = 1 - \frac{Var_{X_i}(\mathbb{E}_{X_i}[Y|X_{\sim i}])}{Var(Y)}$$

SOBOL accepts a list of parameter names and a list of range of values to sample from, which the user can input in the SOBOL settings tab, Figure 3.7a. If no values are added, the parameter is not included in the simulation and the default value is instead used. The user then needs to select the number of samples to run, using the formula 2^x , where x is the number they input, and 2^x is the number of samples that SOBOL will create and run. The larger x is, the more accurate the SOBOL analysis results will be, but the more simulations would need to be run. If 2nd order is not chosen, the model is run $N(D + 2)$ times. If the user wants to analyze the second order interactions, then the model will run the system $N(2D + 2)$ times with the randomly sampled input values, where N is a multiple of 2, and D is the number of parameters being tested. Due to the randomness of the sampling method, the user can, but does not need to, submit a seed value.

Three SOBOL analyses are included by default in the dashboard, as shown in Figure 3.7b. An analysis of the final value of the simulation, the average population count, and the variance in population count. The global and first sensitivity are shown next to one another, and each sub-row within a plot represents each agent type. The proportion of the global and local sensitivity can be seen for each agent type and each parameter.

It can be argued that the final, average, and variance value of the run is not a useful statistic to measure and run a SOBOL analysis on. One might give the reasoning that the population value at time t depends on the previous time step $t - 1$. Thus the average and variance of the value is not completely random and is semi-dependent on the previous value. Another argument is that the simple Golding model doesn't exhibit complex behavior unlike the oscillating behavior exhibited in Figure 2.4.

Making a dashboard that can be used for different inputs is hard to make. Predicting the type of plots that a user might be interested in, and the type of behavior the user wants to analyze is impossible to predict. Therefore, three simple and easy to understand default SOBOL analysis methods are provided that aims to capture the simple dynamics of the system. Upon completion of a SOBOL analysis, the original simulation data is saved to the disk as a *.pickle* file so that the user can reuse the data and run their own SOBOL analyses.

Ultimate Analysis The Ultimate Analysis section does not produce any visualizations or analysis, but instead allows for the user to define which ICs and parameter values they want to run a simulation on. The solver will iterate over every single parameter input possibility and save the results in a *.parquet* file. Similarly settings in the other sections, the user can specify a start and end value, along with the number of values to generate evenly spaced within that range, including both the start and end

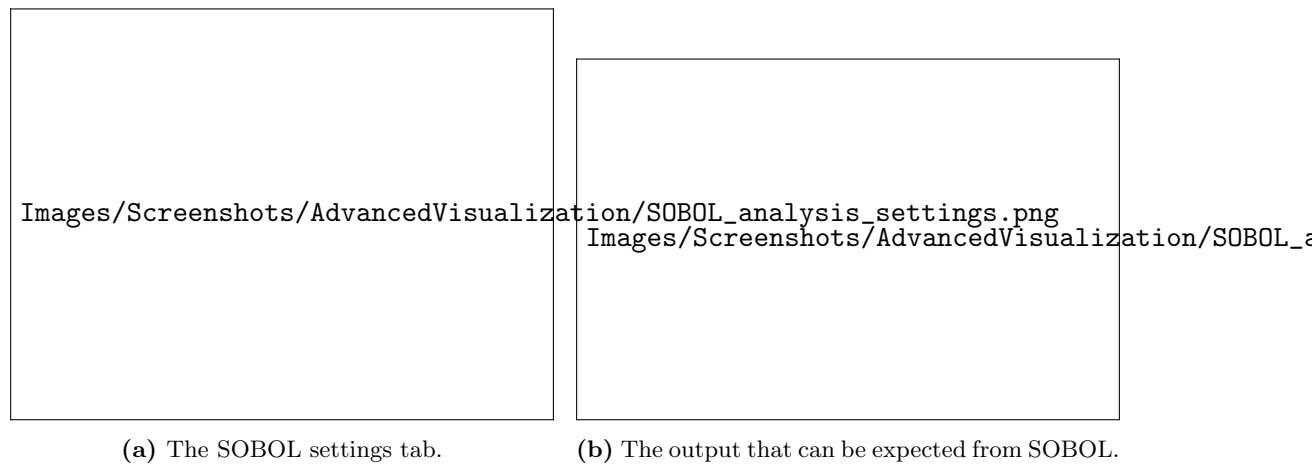


Figure 3.7: SOBOL variance analysis settings and output.



Figure 3.8: The ultimate analysis setup tab.

values (Figure 3.8).

Using Dask and the saved *.parquet* file, the user can query for specific runs, for example runs where a parameter value was greater than 0.05, and use the simulation data to create their own plots.

3.1.4 Custom Visualizations and Analyses

The final part, an optional step, allows the user to define a number of parameters they want to simulate and download the simulation results. The user can use this data to create their own custom visualizations without having to rerun the simulations, especially if there are many simulations. The data can be further processed and visualized as the user wishes.

Depending on the provided model, different behavior might appear. As the dashboard can not create a graph for every situation, or be easily adapted to analyze every situation, Ultimate Analysis can be used to run and download the simulation data to the disk to later create your own custom visualizations. For example the agents in a model can exhibit cyclic behavior. A custom visualization that could be created for this cyclic model would be to perform a Fourier transformation on the curve to obtain the predominant frequencies. A change in parameter values would change the frequencies of the curve, so it would be easy to quantify how a change in parameter value affects the frequency output. If dampening occurs, then a change in amplitude can also be measured, and compared to the change in frequency, allowing the user to identify if the frequency-dampening relationship is correlated or not.

3.2 The Golding Model

The default model, the “Golding model“, sourced from Geng et al. [21], describes the interactions between Resources, Uninfected bacteria, Infected bacteria, and Phages. All plots and simulations will use this model.

3.2.1 The Golding Model

where R is resources, U is uninfected bacteria, $I_{1,\dots,M}$ is the infected stage of the bacteria, and P is the phage population.

The model describes three biological processes, cell consumption of resources and growing, phage/cell encounters and infection, and cell lysis. The cell growth process is described by $g(R, v, K)$, the instantaneous growth rate dependent on the Monod equation, where v is the maximal growth rate and K is the Monod constant. The consumption rate of a resource by a bacteria is e .

Once infected by a phage, the bacteria goes from U to I_1 . The bacteria goes through M stages of infection I_1, \dots, I_M before lysing, where the bacteria goes from state I_k to

Equation 3.6 The Golding model sourced from Geng et al. [21]. The text in **red** has been added to the model, adding (the wash-in) fresh resources (ω^i) and the removal (wash-out) of agents (ω^o). The washin is not dependent on the current resource population, as it is a constant rate being added. By default these values are 0. A summary of the parameters can be found at Table A.1.

$$\frac{dR}{dt} = -e \cdot g(R, v, K) \cdot (U + \sum_{k=1}^M I_k) + w^i - w^o \cdot R \quad (3.1)$$

$$\frac{dU}{dt} = g(R, v, K) \cdot U - r \cdot U \cdot P - w^o \cdot U \quad (3.2)$$

$$\frac{dI_1}{dt} = r \cdot U \cdot P - \frac{M}{\tau} \cdot I_1 - w^o \cdot I_1 \quad (3.3)$$

$$\frac{dI_k}{dt} = \frac{M}{\tau} (I_{k-1} - I_k) - w^o \cdot I_k \text{ for } k = 2, \dots, M \quad (3.4)$$

$$\frac{dP}{dt} = \beta \cdot \frac{M}{\tau} \cdot I_M - r \cdot (U + \sum_{k=1}^M I_k) \cdot P - w^o \cdot P \quad (3.5)$$

$$g(R, v, K) = \frac{v \cdot R}{R + K} \quad (3.6)$$

state I_{k+1} with equal transition rate $\frac{M}{\tau}$. The probability of a successful infection of a cell is r . After a bacteria lyses after stage I_M , β phages are released, the burst size of the phage.

However this model is specifically designed for a $1 \times 1 \times 1$ model. In order to adapt this model to fit an $p \times b \times r$ model, the model needs to be slightly adapted. There are other changes that can be made to the model, for example by adding a washin rate ω^i , where resources are constantly being introduced, and a washout rate ω^o where all agents are washed out at a constant rate. These changes are highlighted in Equation (3.6) in **red**.

3.2.2 The Adapted Golding Model

Equation (3.12) accounts for the interactions of multiple agents, and assumes the interactions occur independent of one another. Each updated population count is a sum of all interactions occurring independently of one another.

3.3 Software Used and Packages

The program was created exclusively in Python [58], and makes extensive usages of various packages, ranging from the standard scientific packages such as NumPy [59] and SciPy to more niche packages such as pickle and SALib [60, 61].

Equation 3.12 Probability of phage infection r_{pb} is not to be confused with R_r , short for Resource r . The interactions are a sum of all interactions due to all interactions taking place at the same time.

$$\frac{dR_r}{dt} = - \sum_{b \in B} e_{br} \cdot g(R_r, v_{br}, K_{br}) \cdot (U_b + \sum_{k=1}^M I_{b_k}) + w_r^i - w^o \cdot R_r \quad (3.7)$$

$$\frac{dU_b}{dt} = U_b \cdot \sum_{r \in R} g(R_r, v_{br}, K_{br}) - U_b \cdot \sum_{p \in P} r_{pb} \cdot P_p - w^o \cdot U_b \quad (3.8)$$

$$\frac{dI_{b_1}}{dt} = U_b \cdot \sum_{p \in P} r_{pb} \cdot P_p - \frac{M}{\tau_b} \cdot I_{b_1} - w^o \cdot I_{b_1} \quad (3.9)$$

$$\frac{dI_{b_k}}{dt} = \frac{M}{\tau_b} (I_{b_{k-1}} - I_{b_k}) - w^o \cdot I_{b_k} \text{ for } k = 2, \dots, M \quad (3.10)$$

$$\frac{dP_p}{dt} = \sum_{b \in B} \beta_{pb} \cdot \frac{M}{\tau_b} \cdot I_{b_M} - r_{pb} \cdot (U_b + \sum_{k=1}^M I_{b_k}) \cdot P_p - w^o \cdot P_p \quad (3.11)$$

$$g(R_r, v_{br}, K_{br}) = \frac{v_{br} \cdot R_r}{R_r + K_{br}} \quad (3.12)$$

The graphical tool uses Tkinter acting as the front end, handling the user inputs, while NetworkX [62] stores the graph and contains the attribute data of the edges and nodes. The GUI tool also uses Matplotlib [63] to create the figure of the graph to display to the user in the GUI tool.

The simulation framework, the backend of the modelling, makes extensive usage of SciPy's *solve_ivp()* to create the ODE data. It also makes light usage of NetworkX to load the graph and parameter values, as it initially takes a graph as an input. NumPy is used to set the parameters up at program startup.

The visualization part makes heavy usage of Dash and Plotly. Dash acts as the server and is used for displaying the HTML aspect of the frontend and dealing with any input and output. Upon choosing parameter values and clicking on “submit“, Dash registers the activity and calls the function registered to the button, sending data such as parameter values and options like “log x-axis” from the frontend to the backend server. In the backend, the various inputs are handled, like changing the input string “0.05, 0.1, 0.15, 0.2” into an iterable list $[0.05, 0.1, 0.15, 0.2]$ that the simulation framework can iterate over to vary the parameter value.

If there are many simulations to run through, in the case of Ultimate Analysis, an intermediate call to a parallel computing library Joblib is called. Joblib parallelizes the computations on multiple CPUs to speed up computing time.

Ultimate analysis uses Pandas to write the data to a *.parquet* file. Pandas parquet offers efficient data compression, efficient memory usage and when combined with Dask, efficient querying functionalities in a Dataframe format that many data scientists would be familiar with.

SOBOL uses the SALib library to sample and analyze the parameter input. Both ultimate analysis and SOBOL save a *.pickle* file containing a dictionary with the parameter values tested, setting values, and other important information regarding the simulation.

Initial Value Analysis uses SciPy's *curve_fit()* function to curve fit the points in the middle plot (Figure 3.5b).

Other packages that are used include collections, copy, warnings, itertools, os, datetime, json, gc, and time.

Chapter 4

Experiments and Results

This section presents the various experimental results obtained.

4.1 Graph Behavior

Table 4.1 elaborates how a change in parameter value changes the shape and population level of the agents. Figure 2.5a is used as the reference graph to compare the graphs. The default values for Figure 2.5a can be found in Table E.1. Each parameter was individually changed to a higher and lower value from the reference value, and the changes are noted in Table 4.1.

4.2 SOBOL Sensitivity Analysis Results

Figure 4.1a shows the impact that the parameter had on the final value of the population at $t = 15$ for a $1 \times 1 \times 1$ system. Figure 4.1b shows the impact that the parameter had on the peak population count, using the 95% rule. Figure 4.1c shows the impact that the parameter had on the time of the peak, using the 95% rule.

The parameters that were tested include all the parameters listed in the basic Golding model, except for Uninfected Bacteria, M , washin, and washout. Uninfected Bacteria was left out as it doesn't make sense to start with infected bacteria to the system, and infected bacteria go from state to state in a constant uniform manner. M , the number of stages that the infection goes through, can not be tested as M hard-codes the array size of the uninfected bacteria before the simulation framework starts. As such, it is not possible to change M without rerunning the program from the very start. The washin rate and washout rate consistently had the largest influence on the final, peak value, and

Parameter	Tested Value	Description of Behavior
R (400)	500	More uninfected and infected, slightly more phages.
	300	Slightly less uninfected and infected, earlier resource depletion.
U (50)	70	Slightly more phages and uninfected and infected bacteria.
	30	Less uninfected and infected bacteria, slower resource depletion, not all resources used, slightly less phages.
P (10)	20	Less resources consumed, less uninfected, bacteria peaks earlier, slightly less phages.
	5	Resources consumed faster, more uninfected, infected, and phages.
τ (2.14)	10	Faster resource depletion, faster bacteria peak, plateau, then fall in population. more uninfected and infected, less phages.
	0.5	Barely any resource consumption, little bacteria growth and uninfected, more phages.
ω^i (0)	15	Slightly more bacteria, resource replenish after bacteria die out.
e (0.03)	0.1	Faster resource depletion, sharper decline in uninfected, less infected and phages.
	0.01	Less resource consumption, slightly more bacteria.
v (1.2)	1.8	More phages, significantly more bacteria, earlier and sharp peak in uninfected.
	1	Less phages and bacteria, less resource consumption, earlier bacteria peak.
K (10)	100	Less resource consumption, less bacteria and phages, earlier bacteria peak.
	1	Faster resource depletion and sudden stop instead of gradual slowdown, earlier bacteria peak.
r (0.01)	0.1	Less consumption, less infected and phages, earlier peak in bacteria..
	0.001	Faster resource consumption rate, more infected and phages, delay in bacteria peak, sharp bacteria peak, small plateau in bacteria count before drop.
β (20)	50	More phages, earlier bacteria peak, less resources consumed, less bacteria.
	10	Faster resource consumption, more uninfected, less phages, sharper bacteria peak.
ω^o (0)	0.02	Faster resource depletion, more bacteria and sharper peak, later peak, and less phages.

Table 4.1: A table that compares how moving one individual parameter value up or down relative to Figure 2.5a changes the general shape of the curve. This table is not meant to be exhaustive, cover edge cases, or extreme cases, or cover every exact detail and change in the population graph, but just to give an idea of how a change in parameter influences the graph shape, such as the rate of resource depletion, maximum number of bacteria and phages, and change in peak time. Reference parameter values used to compare the produced curves are included in the parentheses, taken from Table E.1.

time of peak value, using the 95% rule. Washin and washout significantly skewed the results and analysis and warrants an analysis without washin and washout. The results for a SOBOL analysis with washin and washout can be found in SOBOL Analysis With Washin and Washout.

4.2.1 Final Value Results

4.2.1.1 Resources

The final value for the resources depended heavily on the initial Resource concentration. There weren't many interactions with other parameters because $ST \equiv S1$. e had little influence on the system despite e acting as the link between the resources and bacteria and directly controlling the rate of resource consumption. τ had a larger influence in the final resource value than e .

4.2.1.2 Phages

The final phage population depended on r the most, with β as the second most important parameter influencing the final population value. The other parameters had little to no influence on the final phage population levels.

4.2.1.3 Total Bacteria

The final total bacteria population depended mostly on β , but via many second or higher interactions as noted by $ST \gg S1$. The final population depended heavily on many higher order interactions with Resources, τ , and e . Resources, τ and e was responsible for about 25% of the sensitivity to the output each.

4.2.2 Peak Value Results

4.2.2.1 Phages

The SOBOL peak value plot is basically the same as the final value. Similar to the Final Value Analysis, the phage max value is highly dependent on the value of r and β .

4.2.2.2 Total Bacteria

The total bacteria peak value analysis has similar plot shape. β still has the largest bar graph, but instead of ST and $S1$ being equal to 1 and 0.28 like in the final value, the sensitivity value is only 0.54 and 0.16 respectively. Every parameter plays some influence on the output, but with higher order interactions as for all parameter inputs, $ST > S1$.

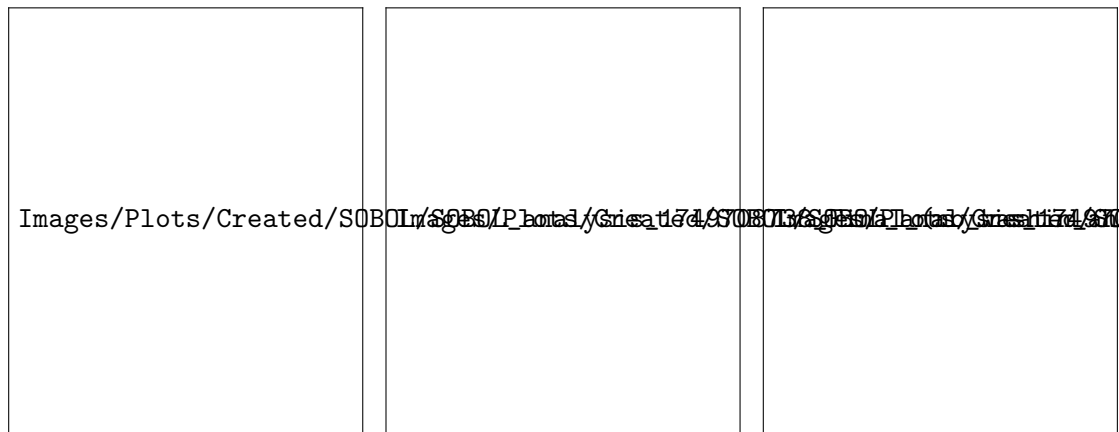
4.2.3 Time of Peak Value Results

4.2.3.1 Phages

With the time of peak value, τ becomes the most important parameter for determining the final phage value and r and β less so.

4.2.3.2 Total Bacteria

β and τ are the two most important factors in determining the time of peak for the total bacteria. The only parameter that does not influence the time of peak is e , otherwise every parameter influences the time at which the bacteria population peaks.



(a) Final value, no washin and washout. (b) Peak population value, no washin and washout. (c) Time of peak value, no washin and washout.

Figure 4.1: SOBOL analyses for the final, peak, and time of peak value, without a washin and washout rate. The input value ranges to test each parameter used for this SOBOL test can be found in Table E.3, except washin and washout was set to 0.

4.3 Initial Value Analysis Results

Figure 4.2a and Figure 4.2b illustrate how varying the initial uninfected bacteria population from 1 to 500 (using 100 different starting values) affects the dynamics and time of peak population of phage and total bacteria populations using the 95% rule.

Figure 4.2a replicates Figure 1 of Mulla et al. [1] perfectly. As the initial bacteria population increases, the time to reach the phage and bacteria sum peak decreases, following $y = -0.8648 \cdot \ln(x) + 9.7911$ and $y = -1.0056 \cdot \ln(x) + 7.7626$, with $R^2 = 0.9800, 0.9988$ respectively.

Figure 4.2b on the other hand shows different behavior. As the initial bacteria population decreases from 500 to 100, the same behavior in Figure 4.2a is noticed. However at 100 and less initial uninfected bacteria, there is a change in behavior. Instead of following the predicted line like in Figure 4.2a, the curve for the phages suddenly decreases, following a quadratic like curve. The bacteria on the other hand plateau before starting to increase again. Both curves resemble a spoon-like shape. A straight handle with a "bowl" to hold the liquid. The fitted curves follow $y = -0.1292 \cdot \ln(x) + 10.1462$ and $y = -0.6234 \cdot \ln(x) + 6.9602$, with $R^2 = 0.5406, 0.9206$ respectively. Despite the large bacteria sum R^2 value, the fitted curve does not fit the data.

4.4 Phase Portrait

Figure 4.3a shows a phase portrait varying the initial resource and phage concentration. For phages that start above 25.98, the phage population can proliferate (until the washout would eventually remove the phages). For phage populations that start below 25.98, the washout removes the phages before the phages had time to infect and kill the bacteria. Both regions of phages exhibit consistent behavior, of either going to 0 or proliferating. If the phage population started at exactly 25.98, if the initial resources was 260 or above, the phages died out. If the initial resources was 255 or below, the phages would proliferate. Expanding on these results by simulating more initial values creates Figure 4.3b. The initial resource values span from 1 to 500, and the initial phage values range from 25.5 to 26.5, each with 100 unique values sampled. Each cell is a unique set of initial conditions. If the phages proliferated for that condition, the box is colored red. In this case, proliferated means that the phage population reached at least 2 times the initial condition. If the box is white, it means the phages died out before being able to reach 2 times its initial concentration. A boundary between the dead and proliferating phages can be curve-fit following $y = \frac{86.756x}{15.811+x} - 10.241$ with an R^2 value of 0.994. Figure 4.3 zooms into the range (1 – 40, 24.2 – 25) for a high detailed view

Images/Plots/Created/IVA/initial_value_analysis_UB_50_500_a_good_plot_2.png

(a) IVA for Table E.2. Replicates Figure 1 of Mulla et al. [1]. The system is adsorption limited [1].

Images/Plots/Created/IVA/initial_value_analysis_UB_50_500_a_good_plot.png

(b) IVA for Table E.1. For uninfected bacteria less than 100, the phage-bacteria interaction is resource limited.

Figure 4.2: Varying initial Uninfected Bacteria concentration, from 50 to 500, with 30 unique values tested over two different instances of "good" curves. Even with two "good" curves, even varying the default parameter values a tiny bit can have a large influence on how changing the initial bacteria concentration can have an influence on the dynamics of the system, changing the behavior of the peak time. The default values for Figure a) and b) can be found at Table E.1 and Table E.2.

of the behavior happening around initial resources of 10. At about resources of 6 or 7, there is a minimum in phage proliferation. For initial resource values of 6 or below, as initial resources increase, less phages (although very miniscule changes) are required to proliferate. For initial resource values of 7 or above, more phages (although very miniscule changes) are required to proliferate.

4.5 Plotting Parameter Change - $3 \times 2 \times 3$ Model

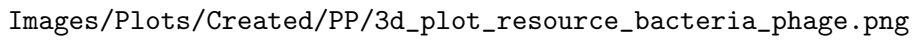
Figure F.3, Figure F.4, and Figure F.5, show a 7×7 matrix of different r and β initial conditions for a $3 \times 2 \times 3$ model, and each figure changes the washout rate from 0 to 0.02 to 0.05. For each simulation, if r or β is equal to a value not equal to inf , as identified by the title above each sub-figure, then each value of r or β has that value. All phage initial values started at 10. This was specifically chosen to highlight how even though the phage values all start the same, and how two parameter values are controlled, the other



Figure 4.3: Varying initial resources and initial phages and the resulting proliferation and fitted proliferation curve. Proliferation is defined as when the phage population reached at least 2 times the initial starting population. This simulation values used can be found in Table E.2, but with washout set to 0.02 instead of 0.

parameter values and unequal network topology has an impact on the population values of the phages. If r or β is equal to *inf*, then the simulation uses the original data as defined in the IC, vector, and matrix section of the dashboard. As a small example for the $3 \times 2 \times 3$ model, when $r = 0.200$, the simulation framework uses $r = \begin{pmatrix} NaN & 0.200 \\ 0.200 & NaN \\ 0.200 & 0.200 \end{pmatrix}$ as the input matrix to the ODE model. When $r = inf$, the simulation framework uses $r = \begin{pmatrix} NaN & 0.11695 \\ 0.144459 & NaN \\ 0.11895 & 0.13065 \end{pmatrix}$ as the data to simulate the interactions with. For the cells that don't have an edge between p and b or between b and r , the data is represented as *NaN*, short for "Not a Number", *np.NaN*,

The columns and rows of each figure makes it easy to compare how a change in parameter value affects the curve, while keeping the other parameter the same. In $r, \beta, \omega^o =$



Images/Plots/Created/PP/3d_plot_resource_bacteria_phage.png

Figure 4.4: 3D plot of phage proliferation, dependent on initial resource, uninfected bacteria, and phage population. Color scaling from white to red, color is dependent on the max phage population reached.

$inf, inf, 0$, although not a "good curve" due to limited resource consumption and limited bacterial and phage growth, really shows how the different parameter values for each interaction uniquely affect the growth rate of each agent, especially the phage population (P0=blue, P1=green, and P2=purple). Despite all phages starting at the same population level, within the first two or so time units, P1 has less phages than P0 and P2. P2 has the fastest initial growth rate, as P2 has the most phages until $t = 4$, at which point P1 has a larger phage population. P2 reaches its peak population count before P0 or P1, but despite the slower initial growth, P0 and P1 eventually overtake P2

in total phage population. P2 also actually reaches its peak before decreasing in population. There are trace amounts of infected bacteria at the end of the simulation. Since the phage population is reduced by $r_{pb} \cdot (U_b + \sum_{k=1}^M I_{b_k})$, and by specifically choosing the parameter values as used in Table E.4, behavior that hasn't been seen in a $1 \times 1 \times 1$ system has been found. The complete extinction of the bacteria has been delayed long enough such that at trace amounts, there is phage reduction despite bacteria still existing. The peak times for P0, P1, and P2 are $t = 6.33, 7.99, 4.52$, a difference of 3.47 time units.

Contrast that with the phage population dynamics of that with $r, \beta, \omega^o = \text{inf}, 100, 0$, the phage populations do not show interesting dynamics. The peak times are more similar and consistent to one another ($t = 5.50, 7.01, 6.78$, a difference of 1.51 time units). The phage population curve all appear the same, with slightly slower growth rates. There is no crossing of phage populations unlike with $r, \beta, \omega^o = \text{inf}, \text{inf}, 0$.

Losing the change in β values really affected the dynamics for the phage population. The highlighted example demonstrated the dynamics and influence that multiple agents can have on the final output.

The top row of Figure F.4 shows how the phages and resources died out relative to the top row of Figure F.3. Even with a high burst value, the phages could not defeat the pressure from the washout. But by changing the r value from $r = 0.001$ to $r = 0.041$, the phages were able to save themselves and proliferate. Using this knowledge, and the information gained from Phase Portrait, a 3D matrix of phage proliferation can be created. Figure 4.4 shows the matrix of proliferation for varying resource, uninfected bacteria, and phage initial conditions. The color consistently changes from white to red across the resources axis, and less so across the bacteria or phages axis. If spliced along the bacteria axis, there is little difference in the shape of the curve. On the underside of the curve, there is some slight variation in color and if the phages proliferated. When spliced on the Resource values near 1, there is the decreasing edge of Phage-Bacteria phage proliferation as the initial resource concentration approaches 6.

4.6 Phage, Bacteria, and Resource Survivability For a $20 \times 20 \times 10$ System

Finally a large $20 \times 20 \times 10$ system can be created

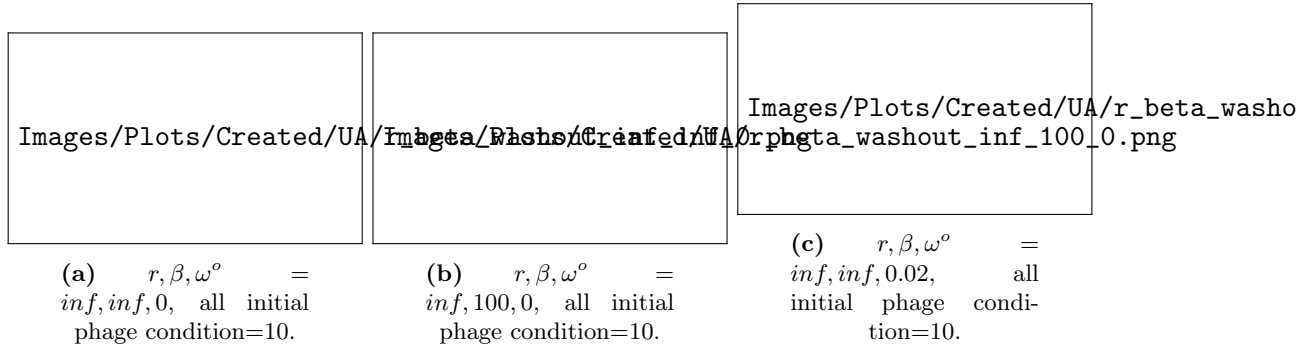


Figure 4.5: Varying r , β , and ω^o . All phage values set to 10 to show how the network connections and vector/matrix values affect phage growth. Selectively chosen sub-figures from Figure F.3, Figure F.4, and Figure F.5. Chosen parameter values can be found in Table E.4.

Chapter 5

Discussion

5.1 Graph Behavior

Table 4.1 presents illustrative examples rather than a comprehensive analysis. The behaviors shown represent typical trends observed when varying each parameter in the specified direction, but they may not apply to all possible values or reflect the magnitude of changes. Additionally, these results do not necessarily generalize to scenarios where two parameters are varied simultaneously. Table 4.1 should be interpreted alongside the local S1 sensitivities from SOBOL Sensitivity Analysis Results to better understand how sensitive the output is to specific parameters and the potential impact of their variation.

5.2 A Good Curve

As the bacterial population grows, resource consumption accelerates until only trace amounts remain at $t = 8$. The delay between the peaks of uninfected and infected bacteria is due to the infection stages and the latent period of phage infection. Each bacterium progresses from infection stage k to $k+1$ at a rate of $\frac{M}{\tau}$. Therefore, decreasing the number of infection steps M or increasing the latent period τ amplifies this delay. A longer latent period means it takes more time for bacteria to progress through the infection stages.

At $t = 4$, the infection rate surpasses the bacterial replication rate, causing the bacterial population to decline even though resources are still available. This moment coincides with the rise of the phage population. Observing the timing of these events and changes in graph behavior, as well as their relationships across different graphs, helps clarify the

complex population dynamics and the interdependence of the populations that might not be obvious from reading the ODE model.

This becomes more difficult when the model goes from a $1 \times 1 \times 1$ system to a $p \times b \times r$ system. Now up to any number of phages can interact with any number of bacteria, and any number of bacteria can interact with any number of resources at varying rates. These varying rates will significantly influence the dynamics of the system, and make it hard to determine what event caused what due to the rise in number of interactions. For a $1 \times 1 \times 1$ system, there are 2 interactions that can occur (assuming no self interactions, and that phages don't interact with the resources). With a $p \times b \times r$ system, there are $\mathcal{O}(p \cdot b + b \cdot r)$ interactions that can occur. So for a $3 \times 2 \times 3$ system, there are at most 12 interactions occurring. 12 events can occur at the same time, making it hard to identify the cause of the event.

5.3 SOBOL Sensitivity

5.3.1 Final Value Analysis

5.3.1.1 Resources

For most simulations, all resources no matter the initial value, will have been used up before the end of the simulation. So on average, the final value for resources will be 0. This explains why the resource sensitivity is so high. There are some combinations of parameters that when chosen, will result in not all the resources being used up. For example, with Table E.2, if $r = 0.2$, not all the resources have been used up. Every parameter affects how the bacteria and phage population grows in some way, which influences the consumption rate of resources, which determines the final resource value. Of the other parameters, τ has the biggest influence because τ determines how fast the bacteria will go through the infection process. The longer it takes, the longer it takes for the phage population to grow, allowing more bacteria to grow and consume resources.

5.3.1.2 Phages

The r value allows the phages to infect the uninfected bacteria. r , the adsorption rate of phages to bacteria, can be interpreted as the efficiency of infection. The smaller the value, the more efficient the infection process is, and fewer phages it requires to infect a bacterium. With a larger r value, more phages are used to infect a bacterium. β has an influence on the final phage population, as the infected bacterium will release β

phages into the system. The more phages that are created for every lysed bacterium, the more phages are available in the system. But larger r values will effectively require more phages to infect the bacterium.

5.3.1.3 Total Bacteria

Resources, τ , e , and β all play a critical role in the final population value of bacteria. More resources allow bacteria to grow for a longer time, allowing more bacteria to be created. τ determines the infection process. The larger τ is, the longer it takes for the bacteria to lyse and create new phages to infect other bacteria. β has a very important role in determining the final bacteria population, but surprisingly r has no role in determining the final bacteria population. e determines how fast the resources are consumed. The larger e is, the faster the resources are being consumed and depleted. So by lowering e , more bacteria will be created, and the time at which the bacteria peak at occurs later in time. Of course as β changes value, it will have a large influence on the final bacteria population. More phages will cause more infections, slowing the spread of bacteria. However, r surprisingly does not have an influence on the final bacteria population level.

5.3.2 Peak Value Analysis

5.3.2.1 Resources

The peak value for resources in always starts at $t = 0$ and is either decreasing or constant, never increasing in concentration. As SOBOL measures the change in initial resource concentration and the resulting max value reached, it associates the initial condition with the peak value.

5.3.2.2 Phages

The barplot values for the peak value for phages using the 95% rule has the same values as in the final value plot for the phages. This makes sense as there is no removal of phages from the system, so any phages created by r or β will stay in the system. As the population is ever-increasing, the final and peak value will be occurring near one another and are tightly associated with one another.

5.3.2.3 Total Bacteria

The total bacteria peak population is much more sensitive to the different parameter values. The bacteria act as a link between the phages and resources. Any changes in the resource consumption rate or initial condition will affect the bacteria population. Likewise, any change in phage adsorption rate will affect the bacteria growth, which in turn will affect the resource consumption rate. The bacteria have the ability to dampen the effect of certain parameters. For example, the initial resource value affects the final resource value. The initial resource value partially affects the final bacteria value, but it doesn't affect the phages. The parameters lose strength as it propagates through the system.

Since the bacteria exist in the middle between the phages and resources, the bacteria are exposed to many different parameters that will ultimately influence the peak value. Many of these parameters are interacting with one another hence why $ST > S1$ is true for many of the inputs.

5.3.3 Time of Peak Analysis

5.3.3.1 Resources

The time of peak value for resources will always be at $t = 0$, and no parameter change can affect that, so SOBOL does not give an output for the peak time of resources

5.3.3.2 Phages

The τ parameter influences how fast an infected bacterium goes through the infection process. Decreasing tau increases the speed of lysis, allowing more phages to be produced faster. This in turn will increase the phage population faster than other parameters, meaning that the phages reached the peak population faster. r and β have similar effects, but rather have a larger effect on the final and peak phage population than the time it takes to reach the peak value. r and β add to the phage population, rather than specifically speed up a process which τ does. Decreasing r and increasing β lead to more phages being created, which can then infect more bacteria. This won't have nearly as large of an impact as shortening the infection period, literally decreasing the time until new phages are created, thus causing the phage population to reach its peak faster.

5.3.3.3 Total Bacteria

Similar to the peak value, the bacteria interact with many parameters, who interact with other parameters. The time of the peak can only occur between $t = 0$ and the end of the simulation, limiting the values that can be measured, reducing the potential variance seen in the output. The peak value on the other hand has no limit on the peak value, with a peak value occurring anywhere between 0 and ∞ . e and K depend almost exclusively on higher order terms due to the nature of the bacteria growing at the Monod rate.

5.4 Initial Value Analysis

The behavior between Figure 4.2a and Figure 4.2b should be similar, however the change in parameter values altered the simulation to introduce a region in behavior change. It would be expected that for 100 initial uninfected bacteria and less the bacteria sum peak time would follow the linear regression line, but at around 100 uninfected bacteria and less, the peak curve deviated from the linear expression.

Between 100 and 500 uninfected bacteria, the system is adsorption limited. The adsorption of phages to bacteria depends on the bacterial concentration [1]. There are not enough phages relative to the population to infect the bacteria, so the phages slowly adsorb to the bacteria. The bacteria can grow without immediate pressure from the phages. There is also a lack of resources which is restricting the bacterial growth. For large initial bacteria concentrations, the resources run out. This severely limits the ability for the bacteria to grow and artificially limits the population cap of the bacteria.

The system is latency limited between 25 and 100 uninfected bacteria. The collapse time in a latency limited regime is independent of the initial bacteria population [1]. As the initial bacteria decreases, the phage to bacteria ratio increases, and they can infect the bacteria faster. So the time to phage peak also decreases as the initial uninfected bacteria decreases.

As the uninfected bacteria decreases from 25 towards 1, it takes longer for the bacteria to grow and reach their peak population count. At these initial bacteria concentration levels, there is enough resources to fully sustain the bacteria through the whole simulation. For uninfected bacteria less than 25, the system enters a new sort of restriction, where the system experiences a delayed in infection due to low encounter rates. The transition rate from U to I_1 is proportional to $U \cdot P$. With low U , less bacteria are initially infected. If the phages can't infect the bacteria, the later infection stages are delayed

due to the slow infection process. There could be a threshold for phage to uninfected bacteria where a certain dilution rate will significantly affect the peak time. This value could be around $\frac{\text{initial phage}}{\text{initial bacteria}} = \frac{10}{25} = 0.4$ as at around 25 uninfected bacteria is when the system switches from latency limited to the new limited regime. The bacteria have a longer amount of time to grow as there is a low infection rate and plenty of resources to consume. This means that it takes longer for the bacteria to grow, as noticed by the increase in peak time relative to larger initial uninfected bacteria populations. As the bacteria population drives the phage population, an increase in bacteria time of peak causes an increase in phage time of peak.

5.5 Phase Portrait

There is non-linear trade-off between initial resources and initial phages when there is washout included. The washout non-linearly affects if the phages proliferate or not. The higher the washout, the harder it would be for the phages to proliferate. Phage populations are coupled to bacteria populations which are coupled to resource populations. By varying the initial resource concentration, the bacteria growth rate is affected.

For low initial resource concentration values, values below 10 the resource, the monod curve is below the half-velocity constant (the velocity v is 1 and K is 10). The bacteria are restricted by the resources and can't grow quickly. So more phages are needed to grow. As N increases towards $K = 10$, the bacteria can grow faster. Since K is small, a small change in R causes a relatively large change in the monod rate. This is noticed by the very steep downward line to the left of the minimum.

At around the minimum, the behavior changes. At $R \equiv 6$, the monod rate reaches half of its max velocity. It should be 10, but the washout must have an effect on the monod rate, artificially shifting the point where the half velocity occurs from $K = 10$ to $K = 6$.

As R increases from K , the bacteria are not limited by the nutrients anymore and can grow faster. However, as R increases beyond K , each additional unit of R results in a diminishing increase in the Monod rate, which asymptotically approaches its maximum velocity. As bacteria grow according to the Monod equation $g(N, v, K)$, the phage population dynamics remain tightly coupled to bacterial growth.

Phage proliferation becomes a race against time. If the phage growth rate is not fast enough to initially beat the washout removal rate, or the infected bacteria are washed out before lysing, the phages can not proliferate.

5.5.1 3D Plot

It is not possible to see inside the matrix, but using the color on the outside can give some insights into the behavior happening inside the matrix. Even with the added bacteria, the phage proliferation boundary is still heavily dependent on the initial phages and initial resources, and less so on bacteria.

5.6 Plotting Parameter Change

Chapter 6

Conclusion and future work

6.1 Conclusion

6.2 Future Work

Next steps would be to give the model to the lab technicians running lab experiments so that they can verify the results as seen in the output by comparing the lab results with the model output. With the lab results, the model can be adapted to better fit the lab results. This can be done by changing parameter values, or by changing the model equation. The user can decide to add the Monod microbial growth model to the growth of the bacteria, or adapt the Monod equation to being dependent on multiple sources. Using the model, the technicians can improve and validate their methods. If the empirical results significantly deviate from the model results, the technician can review to see if their method is good. They might have accidentally not added enough resources, or accidentally miscalculated the initial concentration of bacteria.

6.2.1 Other Models

“All models are wrong, but some are useful” — George E. P. Box

This quote could not be more true for modelling phages and bacteria. There are numerous considerations to account for, and there are numerous ways to go about the considerations. Each model has its pros and cons. Take the exponential population

growth model

$$\frac{dP}{dt} = rP \quad (6.1)$$

$$P(t) = P_0 e^{rt} \quad (6.2)$$

where $P(t)$ is the population at time t , P_0 is the initial population, and r is the growth rate. This model acts as a nice introduction to population modelling. It can accurately fit the exponential growth bacteria experience in a petri dish. However, this basic model does not account for a spatial and resource consumption. Eventually the bacteria run out of space and resources, and start to die out. A population can not grow exponentially forever, the resources can only support a maximum population, the carrying capacity. The model can be adapted to include a carrying capacity (the max population level that can be reached), where the new updated model is

$$\frac{dP}{dt} = rP \left(1 - \frac{P}{K}\right) \quad (6.3)$$

$$P = \frac{K}{1 + \left(\frac{K - P_0}{P_0}\right)e^{-rt}} \quad (6.4)$$

where K is the carrying capacity. This adapted model, the logistic growth model better accounts for the eventual restriction of population growth.

Figure 6.1 shows how the carrying capacity has a large influence on the speed and growth trajectory of a population. The logistic curve initially follows the exponential curve before the maximum growth rate is reached and starts to slow down and taper off as the population asymptotically approaches the carrying capacity $K = 200$.

A further step would be to introduce competition between other bacteria. For example, a $p_{0,1} \cdot P_0 \cdot P_1$ term can be subtracted from the logistic growth curve. This term accounts for competition between Populace 0 and Populace 1, with $p_{0,1}$ being the interaction factor between P_0 and P_1 . Assuming P_0 is being looked at and P_0 has a high value, if P_1 is high, then a lot of P_0 is going to die out due to the competition with P_1 . If P_1 has a low population, then not many P_0 are going to die out due to less competition with P_1 .

The model can be further extended by accounting for temperature, pH, more interactions between other agents, the constant addition and removal of other agents, and other considerations.

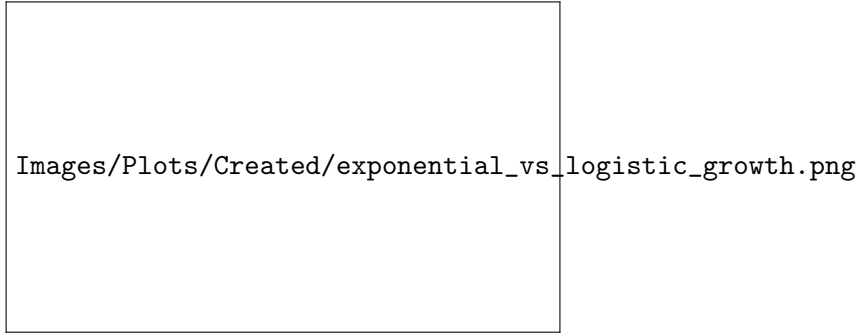


Figure 6.1: Exponential growth curve vs logistic growth

6.2.1.1 Spatial simulations

<https://www.sciencedirect.com/science/article/abs/pii/S0022519318305368> The ODE models work very nicely when there is no consideration for space and 2D/3D-space dimensionality. Spatial models complicate the simulation, making it harder to analyze. Data collection and analysis becomes harder. Unique and novel analysis and visualization methods have to be created to be able to represent and visualize the data through space and time.

PDE PDE are the next logical step to add space to an ODE model. The general formula, as given by

$$\frac{\partial u}{\partial t} = D\nabla^2 u + f(u, x, y, \dots, t)$$

where $u(x, y, \dots, t)$ is the population density of interest, D is the diffusion constant, ∇^2 is the derivative of each spatial direction, and $f(x, y, \dots, t)$ is the function encapsulating growth, death, and interactions dynamics.

Discretization The dimensions can be discretized into boxes of dimensions $\delta x, \delta y, \dots$. This transforms the PDE into a system of difference equations, which can be solved numerically. For example, the Laplacian term $\nabla^2 u$ in 2D can be approximated using finite differences as:

$$\nabla^2 u \approx \frac{u_{i+1,j} - 2u_{i,j} + u_{i-1,j}}{\delta x^2} + \frac{u_{i,j+1} - 2u_{i,j} + u_{i,j-1}}{\delta y^2}$$

where $u_{i,j}$ represents the value of u at the grid point (i, j) . This discretization allows the PDE to be solved iteratively over a grid, enabling spatial simulations of population dynamics. Each box can be represented by a matrix, and the population value can be displayed as a heatmap using visualization software.

Chapter 7

Ethics and Data Management

7.1 Ethical Considerations

There are some ethical considerations needed. Phages can be used to treat bacterial infections, and may need to be safely administered under the supervision of a doctor, despite little to no side effects on the patient. Trying to control phages either in food or in the environment by releasing a phage cocktail into waterways could potentially cause issues further down the line if the released solution contains unwanted chemicals. An extra step in the food production will increase food costs and make food production harder to control. The cost to create, maintain, and use phages at an industrial size can become costly and require a lot of energy. Dumping phages into the ecosystem could potentially cause issues if the phage concoction includes resources for the bacteria to use, and can become costly for taxpayers.

7.2 Data Management

All data and results can be found on GitHub. Some simulation data will have to be recreated as the *.parquet* datafiles are too big for GitHub to store. Measures have been taken to label and document the code, datasets, parameter configurations, and for example with Appendix E. Any qualified researcher should be able to replicate, audit, use, and edit the computational experiments and code if needed. This systematic approach to version control and storage aligns with best practices, ensuring that results are both traceable and verifiable.

7.3 Adherence to Codes and Principles

I acknowledge that the thesis adheres to the ethical code and research data management policies of UvA and IvI.

The following table lists the data used in this thesis, with the source code. I confirm that the list is complete and the listed data are sufficient to reproduce the results of the thesis.

Short description (max. 10 words)	Availability (e.g., URL, DOI)	License
Dataset	Simulation Results	MIT
Source Code	Source Code	MIT
Simulation Conditions	Appendix E and text under figures	

Appendix A

Appendix A: Equation Parameters

Parameters used in the various equations.

A.1 Simple/Advanced Golding Model Parameters

A.2 SOBOL Parameters

A.3 Linear Regression Parameters

Variable	Name	Description
P/P_p	Phages agent	Phage population for phage p
U/U_b	Uninfected Bacteria agent	Uninfected population for bacteria b
I_i/I_{b_i}	Infected Bacteria agent	Infected population for bacteria b at stage $1, \dots, i, \dots, M$
B/B_b	Bacteria agent	Total bacteria population for bacteria b , assuming $B_b = U_b + \sum_{i=1}^M I_{b_i}$
R/R_r	Resource agent	Resource r concentration
e/e_{br}	Consumption rate	Rate at which resource r is consumed by bacteria b
β/β_{pb}	Burst size (B matrix)	Lytic burst size for phage p and bacteria b
r/r_{pb}	Successful phage/cell encounter	Probability of a phage p successfully infecting bacteria b
τ/τ_b	Latent period (tau vector)	Time it takes bacteria b to go through one infection stage
v/v_{br}	Maximal growth rate	Growth rate of bacteria b from resource r
K/K_{br}	Monod Constant	Monod constant representing the resource r concentration at which bacteria b grows at half its maximal rate
ω^i/ω_r^i	wash-in rate	Rate of resources r being added
ω^o/ω^o	wash-out rate	Rate of agents being removed, acts on all agents equally
M	Number of infection stages	Number of infection stages that a bacteria goes through, all bacteria agents have the same value for M
t	time	time value

Table A.1: Golding model parameters with variables, names, and descriptions. Subscripts on parameters indicate relationships; for example, e_{br} is nonzero if there is an edge connecting bacteria b to resource r in the network, zero otherwise.

Variable	Name	Description
Y	Univariate parameter output	univariate model output, such as mean μ or variance σ
X	Input vector	Vector of size d , input vector to f
i	Parameter input	Parameter i of input
X_i	Parameter value	Value of vector X at position $i = 1, \dots, d$, the value of parameter i
d	Input size	Size of input vector X
$X_{\sim i}$	Parameter input	All values of X that are not X_i
f	Function f	Arbitrary black-box function describing model
N	Samples	Number of samples, power of 2, 2^x
D	Parameter input size	Number of parameters inputted into SOBOL, $d = X $
ST_i	Global sensitivity	Contribution of parameter X_i to output variance of Y due to interactions with other variables
$S1_i$	First order sensitivity	Contribution of X_i to output variance of Y

Table A.2: SOBOL parameter symbols, name, and description.

Variable	Name	Description
a	Slope	Slope of the linear regression line
c	Intercept	y-intercept of linear regression line
R^2	Regression Coefficient	Coefficient of determination of linear regression fit, quality of regression
x_i	Data point	Data point on the x-axis
y_i	Actual Value	Actual value of data for a given x_i
\hat{y}_i	Predicted Value	Value predicted of equation for a given x_i
\bar{y}	Average Value	Average y value
n	Number of samples	Number of samples being tested

Table A.3: Variable symbol, name, and description used for the linear regression.

Appendix B

Appendix B: Industrial and Real Life Applications of Phages

Due to the nature of killing bacteria, there are numerous applications where a researcher or an organization might be interested in controlling bacterial populations.

A Food Safety Specialist might be interested in introducing a solution containing a high concentration of phages during food production to prevent the spread and growth of *Salmonella* or *E. coli* in the pet food. Alternatively, the Food Safety Specialist might want to promote beneficial bacteria like *Streptococcus thermophilus* used in the production of Emmental cheese, which heat would kill when the milk undergoes the pasteurization process.

A doctor might be interested in providing swallowable pills, more commonly known as phage cocktails, to a patient with a bacterial infection. There is evidence that phage-resistant bacteria are more susceptible to antibiotics, so the doctor might prescribe both medicines to effectively deal with the infection.

An Environmental Protection Officer might be interested to see how they can use phages to stop the spread of *Cyanobacteria* blooms in waterways, more commonly known as blue-green algae, a photosynthetic microscopic organism that is technically a type of bacteria. This would keep waterways safe for boating and swimming activity, aquatic life, and water consumption in farms, factories, and homes.

When there are a few known bacterial strains, a targeted concoction of phages can be used to control the bacterial population growth in any setting, either be it food, healthcare, or environmental. Phages offer properties of microbial control that other methods do not, making them an ideal candidate for some applications.

B.1 Controlling Foodborne Bacteria

Foodborne diseases are one of the primary ways for bacteria to spread to humans and animals. Some bacteria use the food as a vector to infect hosts, while some bacteria will deposit toxins on the food that is then ingested. If consumed in large enough quantities, or further produced in the host, the toxins can be fatal to the host.

Methods exist to control bacterial growth, for example by storing food below 5°C or above 60°C. Bacteria need moisture to grow, so starches like rice will have minimal bacterial growth. Bacteria prefer to live in slightly acidic to neutral pH environments, so having an environment that is extremely acidic like vinegar will prevent bacterial growth. The use of chemical antibacterial agents such as bleach is not desirable due to leaving chemicals on the food, which can be fatal if ingested. Physical agents like heat or radiation can kill bacteria, but at the cost of altering the food quality [64].

For example, *Streptococcus thermophilus* is one of three different bacteria strains used to create Emmental cheese. However, Emmental cheese does not use pasteurized milk, increasing the risk of *E. coli*. Emmental cheese producers can add phages that target *E. coli* to the milk during the production stage, while not affecting the bacteria used to produce the cheese.

B.1.1 Current Applications

Phage cocktails like SalmoFresh™ have been proven to safely reduce *Salmonella* contamination in pet food and raw pet food ingredients [6], as well as in romaine lettuce and bean sprouts [7]. Pet food contains meat and vegetables, where vegetables grown in or on the ground are at risk of *Salmonella* due to contact with soil, manure, compost, and other agricultural runoff from neighboring farms [19]. Figure B.1 and Figure B.2 show how application of phages have reduced the count of *Salmonella* in ingredients used in pet food as well as romaine lettuce and bean sprouts. In Figure B.1, each food group noticed at least a 68% reduction in CFU/g compared to the control when the 9×10^6 phage treatment was applied. There was at least an 80% reduction in CFU/g across all food groups when treated with a 9×10^6 or stronger phage solution. In Figure B.2, the lettuce and bean sprouts noticed a reduction of at least 0.6 log CFU/mL in *Salmonella* count across all temperature ranges. The smallest reduction in bacteria count in lettuce was noticed at 1 hour at 2°C with an absolute reduction in 62.0% between the control and treatment, while the largest reduction in bacteria of 90.0% was found at 72 hours at 2°C. For the bean sprouts, the lowest reduction in phages was found at 1 hour at 2°C with a reduction of 78.1%, and the largest reduction was 90.0% at 25°C after 48

hours. Although these values are still high above food safe, the ability to reduce the *Salmonella* population by at least 62% and up to 90% at different temperatures and incubation periods is impressive and can prolong shelf life, especially for foods that do not have long shelf lives before spoiling due to bacteria. As such, phages can be shown to control the spread of *Salmonella* in food sources and extend the potential shelf life of certain foods.

Images/Plots/Sourced/SalmoFresh_in_pet_food.png

Figure B.1: SalmoLyse[®] reduces *Salmonella* contamination on various food surfaces: Mean and standard error bars shown. Statistical analyses were carried out for each food group independently. Asterisks denote significant reduction from corresponding controls based on one-way ANOVA with Tukey's post-hoc tests for multiple corrections: ** denotes $p < 0.01$, while *** denotes $p < 0.001$ compared to the corresponding controls. There was significant reduction in *Salmonella* on all food surfaces with the addition of SalmoLyse[®] compared to the controls; the mean percent reductions from the control are noted in the boxes above treatment bars. CFU/g D colony forming units per gram. Each letter denotes a food group that was tested with SalmoLyse[®] and compared to a control: A= chicken; B= lettuce; C= tuna; D= cantaloupe; E= ground turkey. Plot sourced from Soffer et al. [6].

Images/Plots/Sourced/SalmoFresh_effectiveness_lettuce_sprouts.png

Figure B.2: *Salmonella* count in a mixture of 5 *Salmonella* strains spot-inoculated (CFU/g) onto a) lettuce and b) sprouts after spraying with a mixture of bacteriophage (SalmoFreshTM) relative to positive controls at 2, 10 and 25C and stored for 1, 24, 48 and 72 h. Plot sourced from Zhang et al. [7]

B.2 Phage Therapy and Antibiotics

Antibiotics are a common way to treat bacterial infections. However, antibiotics are not selective in the bacteria they kill, killing both harmful and beneficial bacteria. This can lead to the development of antibiotic-resistant bacteria, which makes it harder to combat that bacteria in the future. It has also been shown that antibiotics have a negative effect on the gut microbiome and brain development in mice. Phages are an alternative to antibiotics, as they are selective in the bacteria they kill and do not interact with cells or other important biological functions. The rise in antibiotic resistant bacteria can be attributed to the overuse and over-prescription of antibiotics and incorrect usage of antibiotics (for example prematurely stopping) [15]. These actions provide an evolutionary pressure on bacteria to mutate and gain resistance to the antibiotics. The phage therapy can contain any number of different phages that can target specific bacterial infections such as *Streptococcus pneumoniae* with minimal risk of side effects.

B.2.1 Current Applications: Bacterial Infection Control

One active area of research is the use of phages to control bacterial infections. Due to the specificity of phages, they can be used to target specific bacteria strains without affecting other beneficial bacteria. When sick with a bacterial infection, patients swallow antibiotic pills to help the body fight the infection. Antibiotics work by either interrupting intercellular processes like the synthesis of RNA [65], by disrupting the structural integrity of the cell wall [66], or by inhibiting protein synthesis [67].

However, antibiotics are not strain specific and indiscriminately kill gut and other bacteria. Common side effects of antibiotics, although usually not serious, include diarrhea, nausea, and headaches. It has also been shown that the effects of early-stage penicillin exposure in mice has found to have a long-lasting effect on the gut microbiome, frontal cortex gene expression, and amygdala gene expression [16]. Penicillin increases cytokine expression (small proteins used in cell signaling) in the frontal cortex of the brain, modifies the blood-brain barrier integrity, and alters behavior. The mice exhibited an increase in aggression and anxiety-like behavior [68]. Phages can be used as an alternative to antibiotics without the side effects and without affecting the gut biome.

With an increase in antibiotic usage, there has been an increase in antibiotic-resistant bacteria. The World Health Organization has stated that antibiotic resistance threatens the modern medicine and the sustainability of an effective, global public health response to the enduring threat from infectious diseases. Common infections, that previously

would have been easy to treat, are harder to treat, and can increase the risk of disease spread, severe illness, and death [69].

One area of research is exploring how bacteria can exchange traits such as phage resistance and antibiotic resistance. Some bacteria are multi-drug resistant, and don't react with the medicine anymore.

Laure and Ahn [17] showed evidence that *Salmonella Typhimurium* is more susceptible to ampicillin in the presence of phages, and phage-resistance can lead to reduced virulence and decreased antibiotic resistance.

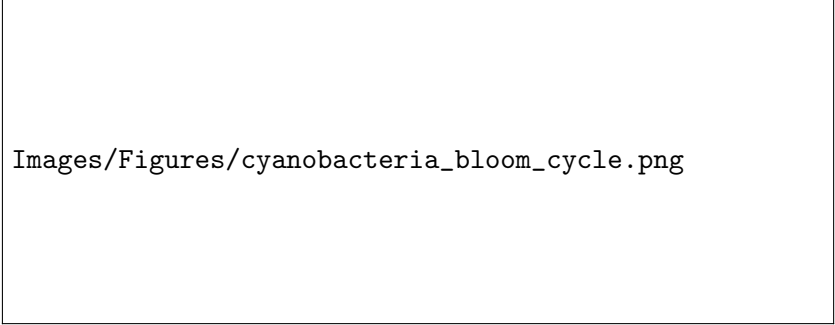
Zhao et al. [18] showed that there exists an antagonist coevolution between the bacteria and phages, where the dynamics changed from an arms race dynamic (ARD) to a fluctuating selection dynamics (FSD). Due to phage selection and bacterial competition pressure, when the bacteria gained phage resistance, it lost antibiotic resistance. A genome analysis revealed mutations in the *btuB* gene of *Salmonella anatum*, with q higher mutation frequency in the ARD stage. A knockout experiment confirmed that the *btuB* gene is a receptor for the JNwz02 phage and resulted in reduced bacterial competitiveness. Further analysis detected multiple single nucleotide polymorphism (SNP) mutations in the phage-resistant strains. The SNPs potentially affected the membrane components, partially weakening the cell defense against antibiotics. These findings help advance our understanding of phage-host-antibiotics interactions and the impact of adaptations to antibiotic resistance. The research shows how phages can be used to reintroduce antibiotic susceptibility to previous insusceptible bacteria, preventing costly and lengthy research in new antibiotics [18].

Phage research is facing challenges due to bacterial strains evolving resistance to phages. Understanding the interplay between antibiotics and phages is essential for shaping future research [18].

B.3 Environmental Protection

Algae blooms, also called red tides, is the rapid spread of bacterial or algae organisms. Blooms are a growing environmental concern impacting water quality, aquatic ecosystems, and human health. These rapid increases in algae populations, often fueled by excess resources like nitrogen and phosphorus, can occur in freshwater, coastal, and marine environment.

Cyanobacteria blooms have major effects on the aquatic environment as well as human health. Cyanobacteria release nitrogen and phosphorous, which the bacteria use to grow



Images/Figures/cyanobacteria_bloom_cycle.png

Figure B.3: Cyanobacteria degradation cycle, main hazards of cyanobacteria bloom to water bodies, aquatic organisms, and the human body. (DO: dissolved oxygen; SD: water transparency; Cond: conductivity; N: nitrogen; P: phosphorus; MCs: micro-cystins). [8]

with oxygen, outpacing other aquatic growth, and killing aquatic marine life. Bacterial toxins can make their way into the food and water consumed by humans, causing muscle fatigue, respiratory issues, liver damage, and gastrointestinal issues [8]. Figure B.3 shows the process of how cyanobacteria degrade and are absorbed into the environment, eventually making their way into the human body via various contact points.

B.3.1 Current Applications

There is interest in using phages to control cyanobacteria blooms. Phages can offer better and safer options than chemical options when trying to control bacterial blooms. Chemical options are indiscriminate, killing cyanobacteria, while also killing other beneficial bacteria and aquatic life, and can eventually seep into groundwater. Although not used to control bacteria blooms, some chemicals like PFAS, also called “Forever Chemicals”, can last a long time in the environment and don’t degrade and keep on negatively affecting the environment. Due to the specificity of phages, only the cyanobacteria will be targeted, and will not affect the surrounding environment.

Tucker and Pollard found that an isolated phage cocktail collected from Lake Baroon in Australia could decrease the abundance of *M. aeruginosa* by 95% within 6 days in a lab setting, before recovering within 3 weeks time [14].

There is evidence that phage-resistant bacteria can influence the population dynamics of other bacteria. It has been shown that the plankton level has been experimentally affected by the frequency of the phage-resistant *Nodularia* marine bacteria. Populations with high phage resistance (> 50%) dominate the plankton communities despite a high phage count and eventually out compete other bacteria due to their slower loss in population count. Contrastingly, populations of bacteria with low phage resistance (between 0% and 5%) were lysed to extinction, releasing resources like nitrogen. This

allows for other bacterial strains to absorb the resources and dominate the bacterial community. Phages and the lysis of bacterial strains can have a dramatic effect on community dynamics and composition of other agents like phages, bacteria, and resources [13]. Phages have the potential to be used as a highly specific strategy for the control of cyanobacterial blooms, with minimal effects to the environment, and offer control of bacterial blooms, with limited impact to the environment. Usage should be relatively safe, novel, efficient, and sensitive.

However, there are issues with using phages to control bacterial blooms. Bacterial blooms can cover vast areas, or be in areas that would be hard to reach like marshlands, applying phages to combat the bloom might be infeasible. If the method of choice was to spray a solution of water containing phages, the solution needs to be shipped to the site and loaded onto special boats to spray the solution into the water, or the trucks need to drive along the shore and spray the solution into the water.

The phage density in the solution will have to be relatively high to quickly combat the bloom. These problems provide major logistical problems with creating the phages in a lab or factory, transporting the phages, and finally the administration of the phages to the waterways. Phages can only diffuse through the water, and can't actively swim, so they are dependent on the rate of diffusion and water currents. This will be difficult in marshlands, where the bacteria can "hide" in the grass and crevices created by aquatic life. If the bloom is in a high current area, like in a river or a bay, the water can wash the phages away.

Scientists have not yet fully understood the phage infection mechanism, and research into the artificial engineering of phages is limited, making it challenging to conduct studies in this area [70, 71].

Algae can produce toxins that threaten wildlife, contaminate drinking water, and disrupt local economies dependent on fishing and tourism. In the state of Florida, between the years 1995 and 2000, the restaurant and hotel industry lost an estimated \$6.5 million to algae blooms. This accounts for about 25% of the average total monthly sales revenue in the region from June through October, the months that are most commonly affected by red tide[72]. During a red bloom event, hospital diagnoses in the county of Sarasota for pneumonia, gastrointestinal, and respiratory illness increased by 19%, 40% and 54% respectively [73, 74], with a respiratory illness visit costing between \$0.5 and \$4 million [75].

Appendix C

Appendix C: Flowchart of User and System Interactions

Figure C.1 shows how the user can interact with the system, the input and outputs for subsystems, and the systems working with one another. To read the flow chart, start from the top to the bottom. First the user creates a network using the GUI Network Creation Tool. After the graph is finished, the user provides an implementation of the network as an ODE model, using Python. Once finished, the user provides the network file and ODE model to the ODE solver. The solver uses information from the network file to determine the number of agents to create, parameter details (including names, values, and dimensions), and setting values. Then the user interacts with the Visualization Dashboard Tool, for example by clicking on buttons to run simulations, changing parameter values, (un)selecting checkboxes, and zooming in and out of plots, and hovering over plots to show data. Once a user has selected the parameter values, the parameter values are sent to the solver. The solver calculates the time and population values using the provided graph and ODE model and sends the data back to the Visualization Dashboard Tool, which then outputs the visualizations. If the user has run an ultimate analysis, then the user can query the saved data to make their own custom visualizations.



Figure C.1: The flowchart of user and system interactions. Read from top to bottom.

Appendix D

Appendix D: ODE Model Implementation

The code listed here is the implementation of Section 3.2.2.

Appendix E

Appendix E: Parameter Values Used

E.1 A Good Curve

IC					
Resources	Uninfected Bacteria		Infected Bacteria		Phages
400	50		[0 0 0 0]		10
Vector Data					
τ	ω^i				
2.14	0				
Matrix Data					
e	v	K	r	β	
0.03	1.2	10	0.01	20	
Environment Data					
M	ω^o				
4	0				

Table E.1: The parameter values used for Figure 2.5.

E.2 A Good Curve 2

E.3 SOBOL Analysis

E.4 Complex Model

Images/Plots/Created/a_good_curve_linear.png

(a) A second curve for "a good curve", linear y-axis.

Images/Plots/Created/a_good_curve_logarithmic.png

(b) A second curve for "a good curve", logarithmic y-axis.

Figure E.1: The log plot allows to see behavior happening at values near 0 and to plot data on a logarithmic scale. The parameters used for this plot can be found in Table E.1.

IC						
Resources	Uninfected Bacteria			Infected Bacteria		Phages
200	50			[0 0 0 0]		10
Vector Data						
τ	ω^i					
0.7	0					
Matrix Data						
e	v	K	r	β		
0.12	1	10	0.001	10		
Environment Data						
M	ω^o					
4	0					

Table E.2: Another set of "good" curves. The linear and logarithmic plot of this data can be seen in Figure E.1

IC					
Resources	Uninfected Bacteria		Phages		
1-500	1-100		1-50		
Vector Data					
τ	ω^i				
0.5-3.5	0-100				
Matrix Data					
e	v	K	r	β	
0.05-0.25	0.8-1.9	10-250	0.001-0.2	1-100	
Environment Data					
ω^o					
0-0.1					
Other Data					
Seed Value	2nd Order	Number Samples		Simulations Run	Simulation Length
0	False	15		$2^{15}(11 + 2) = 425984$	15

Table E.3: The parameter values used for the SOBOL sensitivity analysis in Figure F.1, ?? and Figure 4.1.

IC								
Resources			Uninfected Bacteria		Infected Bacteria		Phages	
[236 287 270]			[53 69]		$\begin{bmatrix} 0 & 0 & 0 & 0 \\ 0 & 0 & 0 & 0 \end{bmatrix}$		[10 5 8]	
<hr/>								
Vector Data								
τ_b			ω_r^i					
[2.73340 2.25015]			[0 0 0]					
<hr/>								
Matrix Data								
e_{br}			v_{br}					
$\begin{bmatrix} 0.15680 & 0.10871 & NaN \\ NaN & NaN & 0.18009 \end{bmatrix}$			$\begin{bmatrix} 1.27601 & 0.86393 & NaN \\ NaN & NaN & 1.22625 \end{bmatrix}$					
K_{br}			r_{pb}			β_{pb}		
$\begin{bmatrix} 139.58353 & 12.83058 & NaN \\ NaN & NaN & 82.86684 \end{bmatrix}$			$\begin{bmatrix} NaN & 0.11695 \\ 0.144459 & NaN \\ 0.11895 & 0.13065 \end{bmatrix}$			$\begin{bmatrix} NaN & 15 \\ 34 & NaN \\ 11 & 57 \end{bmatrix}$		
<hr/>								
Environment Data								
M			ω^o					
4			0					

Table E.4: The parameter values used for the $3 \times 2 \times 3$ network model rounded to 5 decimal points. If there is no edge between agents, then in the matrix representation of the parameter, *NaN*, short for Not a Number, is stored in the matrix data.

Appendix F

Appendix F: Extra Plots and Figures

F.1 SOBOL Analysis With Washin and Washout

F.1.1 Final Value Analysis

F.1.1.1 Resources

Despite the resource consumption rate directly depending on e, v and K , the parameters had very little influence on the final value as evidenced by the ST and S1 bar being near 0. The resource population was mainly driven by the washin and washout value. The peak resources are driven completely by the washin rate. Not many interactions between two or more parameters were occurring.

F.1.1.2 Phages

The most important factor for the final phage value is r , followed by β and ω^o . The other parameters had little to no effect on the final phage value.

F.1.1.3 Total Bacteria

The sum of uninfected and infected bacteria depended heavily on higher order interactions as $ST_i \gg S1_i$. Although not shown, the bar plots for the total bacteria resembled that of the bar-plots for the uninfected bacteria, and less that of the infected bacteria.

F.1.2 Peak Value and Time of peak

To create the custom SOBOL analyses, the peak value and the time at the peak of the population is measured and analyzed. The peak is defined as the point where the population reaches 95% of its absolute maximum value. The time at peak is measured at the point in time that the population reaches 95% of the maximum value. This removes unintended side effects of the simulation. For populations that are only increasing in value, this prevents the measured peak from bunching up at the end of the simulation, skewing the data. As the peak is defined at 95% of the absolute maximum value, populations that have a faster increase on population count at the end will have a time value closer towards the end of the simulation. For populations that reach a plateau, the 95% rule will push the peak time towards the beginning of the simulation, while still "respecting" the absolute final value since $95\% \approx 100\%$. The 95% rule can fail under certain situations, such as when there is cyclic behavior. See *Why 95%?* for a more detailed explanation on why the 95% rule is used.

The results of the SOBOL peak and time at peak analyses can be seen in Figure F.1b and Figure F.1c. Although some of the bars between the final, peak, and time at peak values are the same, some are different. But overall, similar values can be seen across the the final, peak, and time at peak analyses. The peak infected values are more certain compared to the final infected values, which could be due to the 95% rule removing some of the noise of the simulation. The time at peak values have less error compared to the final and peak value. This is due to the restricted range of values. The time at peak value can only fall somewhere between 0 and 15, the start and end values of the simulation respectively. The final and peak values can fall anywhere between 0 and any value, depending on the IC and how high the population can rise, and how fast the population can fall, *if* the population count falls.

F.2 Why 95%?

The 95% rule helps in the IVA analysis. Due to the solver, when taking the absolute peak value, the same time value can occur. Or in an ever increasing value like phages, the peak values occur at the last time step of the simulation, or plateaus and doesn't grow anymore. However, as the parameter value is changing, each graph for every input change will change the growth rate of the agent, changing how fast the agent population grows.

Figure F.2 shows how using the 95% rule vs the 100% rule for finding the max value reached helps smooth out computational errors from the ODE solver and smooths out

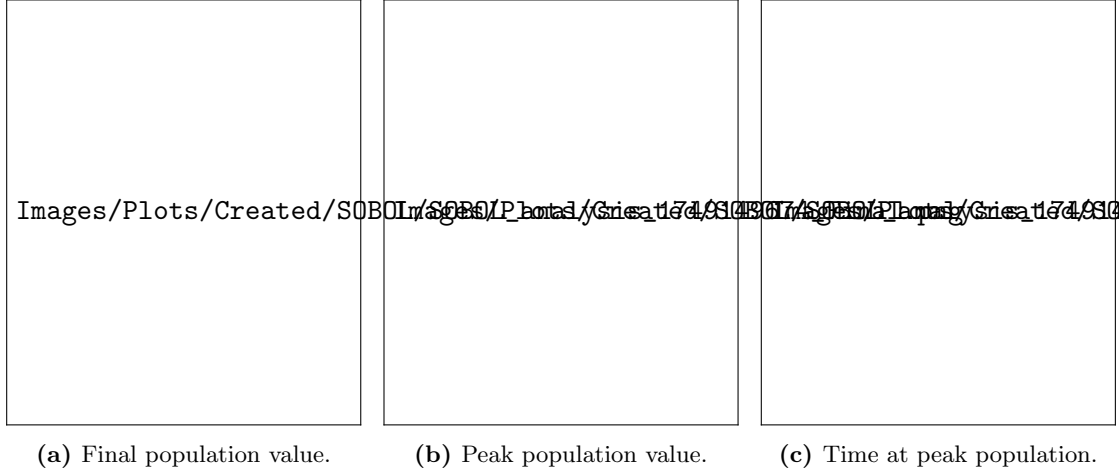


Figure F.1: SOBOL analyses for the final, peak, and time of peak value with a washin and washout rate. The data was saved from the dashboard and plotted using Matplotlib. The values used for this SOBOL test can be found in Table E.3. The data used in Figure F.1a was used for Figure F.1b and Figure F.1c.

the shape. For the phages, using the 100% rule (Figure F.2b) shows that the population peaked at the end of the simulation, $t = 15$, for all e values. However at $t = 15$, the population plateaued, as evident by the line graph. Plotting the same plot, but calculating the peak at 95% of the actual peak (Figure F.2a) shows that the green line ($e = 0.25$) "reached" its peak at $t = 8.4$ before the red line ($e = 0.05$) at $t = 9.4$, a full unit of time after $e = 0.25$. The user can thus conclude that for this instance, larger e values will cause the phage population to reach its "peak" faster than smaller e values.

Figure F.2c and Figure F.2d likewise show how the 95% rule can improve analysis of the change in peak time. Figure F.2d shows how apparently the peak is reached at set time values. Due to how `solve_ivp()` from SciPy works, it automatically chooses time values that it thinks would best capture the dynamics of the system without calculating too many steps. The user can control the step size by decreasing the absolute and relative error bounds, as well as by minimizing the time steps. The user can also provide their own time range with the number of steps to run, increasing the control of the time values chosen. It takes about 0.02321 seconds to run a simulation for 15 time units, where 200 time steps are selected and solved by the solver. Comparatively, a simulation with 1000 time units and 1000000 (a 5000x increase in samples) equidistant time samples takes about 1.71651 seconds to run, a 73.95562258x increase in time spent computing the simulation. The total time taken to run the whole method call, a call to the simple graph maker at the top of the dashboard took 1.76130 seconds vs 17.70634 seconds.

Alternatively instead of controlling the solver, the user can use the 95% rule. Although some accuracy is lost. Going from the 100% rule to the 95% rule, the solver still captures the peak values and the dynamics, but the accuracy is lost. The 100% rule shows that

for $e = 0.25$, the time the uninfected population reached its peak occurred at $t = 3.2$. But for the 95% rule, the time at which the peak occurred at is at $t = 3.05$. The slope (the a value) and the intercept (the c value) are somewhat similar, with very high and similar R^2 values (0.97), suggesting a good linear fit of the data.

Figure F.2e shows how the by increasing the time sampling to more fine grained results in a more accurate graph. Instead of having the solver choose the time values to test, 1000 equidistant time values were selected between 0 and 15. The solver can more accurately calculate the population values and calculate the proper peak time. Comparing the 100% rule without the custom time values with the 100% rule with the custom time values shows the same time values were calculated. in both, the $e = 0.25$ resulted in a time of peak at 3.2 and for $e = 0.05$, the time of peak occurred at $t = 3.95$. This is in stark comparison to the 95% rule vs 100% rule without the custom time, showing a difference of 0.15 time units. The custom time values also preserved the shape of the curve e -value vs time curve, being almost identical to that of the 95% rule as seen in Figure F.2c and Figure F.2e.

Another issue that arises with the custom time is that it doesn't solve the issue seen with the phages, where the time of peak is at $t = 15$.

The user can control the % rule with a value input on the dashboard. They can select to use the 95% rule, or 100% rule, or even 83% rule if they want by changing the value they use. The user can use their own custom time values, to ensure that they get high quality curves.

F.3 Varying r and β In A $3 \times 2 \times 3$ System

Figure F.3, Figure F.4, and Figure F.5 show a 7x7 matrix of figures, each with a unique parameter set. In each sub-figure, the values of r and β are varied as follows: $r = 0.5, 1.1, 1.7, 2.3, 2.9, 3.5, \text{inf}$; $\beta = 0, 20, 40, 60, 80, 100, \text{inf}$. "inf" in the figures, represented as *np.inf* in the code, the representation of ∞ , represents the original parameter values used in the IC, vector data, or matrix data. Each figure shows the effect of varying the washout rate, with values set to 0, 0.02, and 0.05, respectively. All initial phage values were set to 10. This was done to really show how the different interactions with the bacteria, and the value of the parameters affected the phage growth. The default values for the parameters can be found in Table E.4.

Images/Plots/Created/IVA/initial_value_analysis_Phages_95.png

(a) IVA for phage population, 95% rule

Images/Plots/Created/IVA/initial_value_analysis_Phages_100.png

(b) IVA for phage population, 100% rule.

Images/Plots/Created/IVA/initial_value_analysis_Uninfected_Bacteria_95.png

(c) IVA for uninfected population, 95% rule.

Images/Plots/Created/IVA/initial_value_analysis_Uninfected_Bacteria_100.png

(d) IVA for uninfected population, 100% rule.

Images/Plots/Created/IVA/initial_value_analysis_Uninfected_Bacteria_100_own_time.png

(e) IVA for uninfected population, 100% rule, 1000 equidistant time steps.

Figure F.2: Testing the 95% rule vs the 100% rule, where the time at the absolute peak is taken and plotted in the second plot. A comparison of phages and uninfected bacteria is shown. Verification of the graph shape between the 95% rule graph and a frequent time step with 100% rule can be seen between c) and e). The ϵ value is changed, ranging from 0.05 to 0.25.



Figure F.3: Washout $\omega^o = 0$.

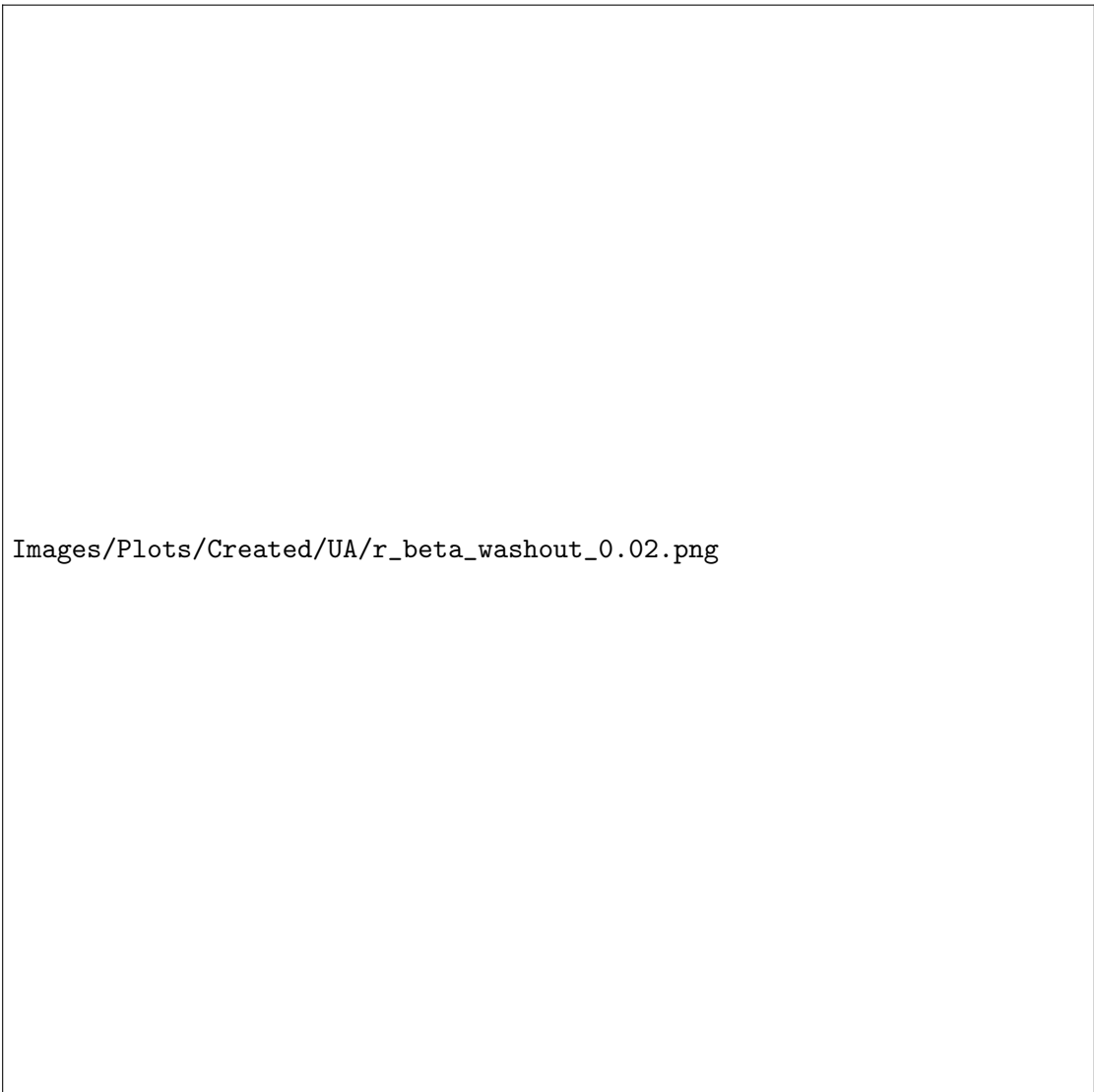


Figure F.4: Washout $\omega^o = 0.02$.

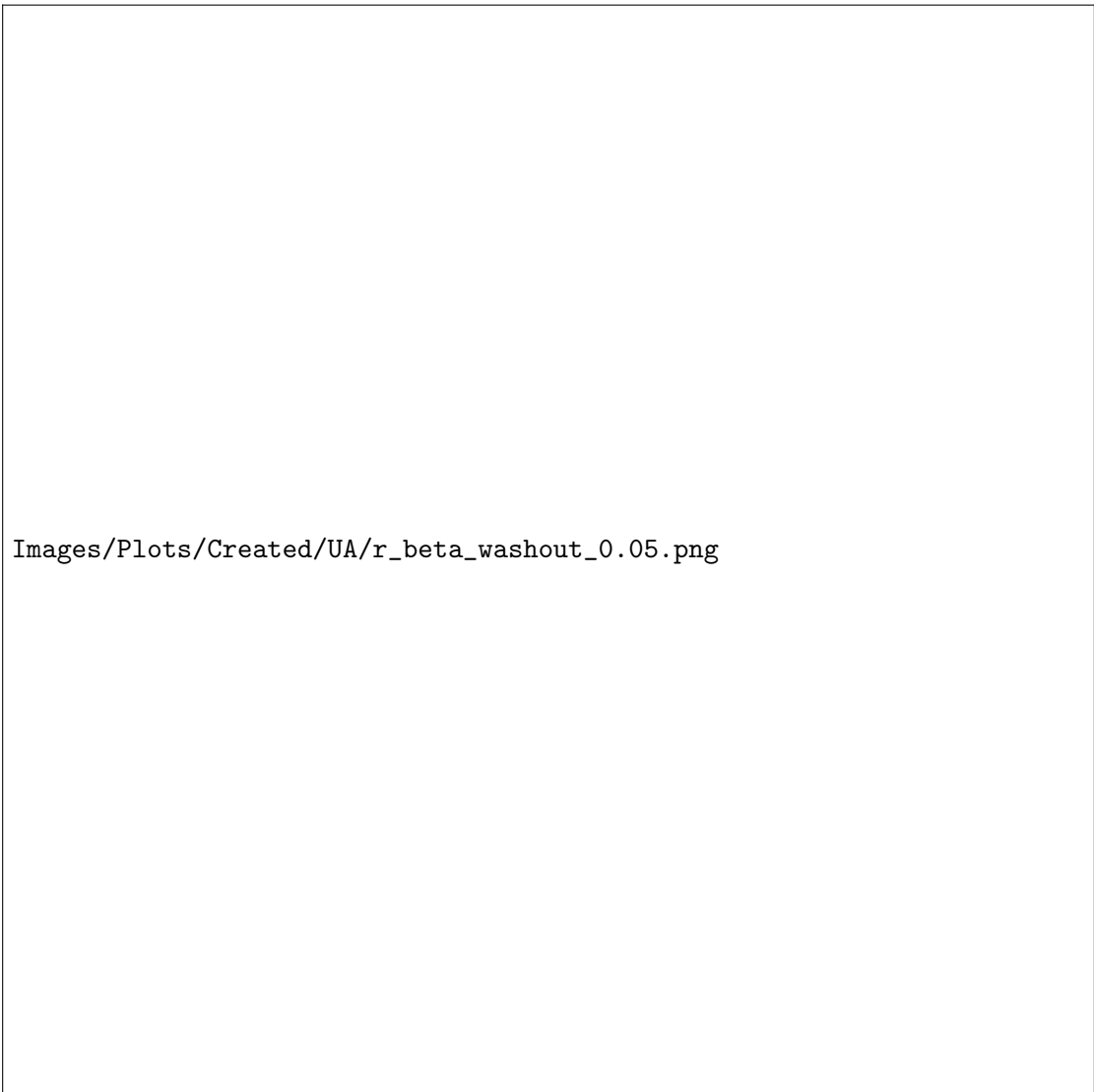


Figure F.5: Washout $\omega^o = 0.05$.

Bibliography

- [1] Yuval Mulla, Janina Müller, Denny Trimcev, and Tobias Bollenbach. Extreme diversity of phage amplification rates and phage-antibiotic interactions revealed by PHORCE, December 2024. URL <https://www.biorxiv.org/content/10.1101/2024.06.07.597930v3>.
- [2] Allan Campbell. The future of bacteriophage biology. *Nature Reviews Genetics*, 4(6):471–477, June 2003. ISSN 1471-0056, 1471-0064. doi: 10.1038/nrg1089. URL <https://www.nature.com/articles/nrg1089>.
- [3] Naomi Iris van den Berg, Daniel Machado, Sophia Santos, Isabel Rocha, Jeremy Chacón, William Harcombe, Sara Mitri, and Kiran R. Patil. Ecological modelling approaches for predicting emergent properties in microbial communities. *Nature Ecology & Evolution*, 6(7):855–865, July 2022. ISSN 2397-334X. doi: 10.1038/s41559-022-01746-7. URL <https://www.nature.com/articles/s41559-022-01746-7>.
- [4] Anders S. Nilsson. Cocktail, a Computer Program for Modelling Bacteriophage Infection Kinetics. *Viruses*, 14(11):2483, November 2022. ISSN 1999-4915. doi: 10.3390/v14112483. URL <https://www.mdpi.com/1999-4915/14/11/2483>.
- [5] Konrad Krysiak-Baltyn, Gregory J. O. Martin, Anthony D. Stickland, Peter J. Scales, and Sally L. Gras. Simulation of phage dynamics in multi-reactor models of complex wastewater treatment systems. *Biochemical Engineering Journal*, 122: 91–102, June 2017. ISSN 1369-703X. doi: 10.1016/j.bej.2016.10.011. URL <https://www.sciencedirect.com/science/article/pii/S1369703X16302728>.
- [6] Nitzan Soffer, Tamar Abuladze, Joelle Woolston, Manrong Li, Leigh Farris Hanna, Serena Heyse, Duane Charbonneau, and Alexander Sulakvelidze. Bacteriophages safely reduce Salmonella contamination in pet food and raw pet food ingredients. *Bacteriophage*, 6(3):e1220347, July 2016. ISSN null. doi: 10.1080/21597081.2016.1220347. URL <https://doi.org/10.1080/21597081.2016.1220347>.
- [7] Xuan Zhang, Yan Dong Niu, Yuchen Nan, Kim Stanford, Rick Holley, Tim McAllister, and Claudia Narváez-Bravo. SalmoFresh™ effectiveness in controlling

- Salmonella on romaine lettuce, mung bean sprouts and seeds. *International Journal of Food Microbiology*, 305:108250, September 2019. ISSN 0168-1605. doi: 10.1016/j.ijfoodmicro.2019.108250. URL <https://www.sciencedirect.com/science/article/pii/S0168160519301709>.
- [8] Weizhen Zhang, Jing Liu, Yunxing Xiao, Yumiao Zhang, Yangjinzhi Yu, Zheng Zheng, Yafeng Liu, and Qi Li. The Impact of Cyanobacteria Blooms on the Aquatic Environment and Human Health. *Toxins*, 14(10):658, September 2022. ISSN 2072-6651. doi: 10.3390/toxins14100658. URL <https://www.ncbi.nlm.nih.gov/pmc/articles/PMC9611879/>.
- [9] Mya Breitbart, Chelsea Bonnain, Kema Malki, and Natalie A. Sawaya. Phage puppet masters of the marine microbial realm. *Nature Microbiology*, 3(7):754–766, July 2018. ISSN 2058-5276. doi: 10.1038/s41564-018-0166-y. URL <https://www.nature.com/articles/s41564-018-0166-y>.
- [10] Basem Al-Shayeb, Rohan Sachdeva, Lin-Xing Chen, Fred Ward, Patrick Munk, Audra Devoto, Cindy J. Castelle, Matthew R. Olm, Keith Bouma-Gregson, Yuki Amano, Christine He, Raphaël Méheust, Brandon Brooks, Alex Thomas, Adi Lavy, Paula Matheus-Carnevali, Christine Sun, Daniela S. A. Goltsman, Mikayla A. Borton, Allison Sharrar, Alexander L. Jaffe, Tara C. Nelson, Rose Kantor, Ray Keren, Katherine R. Lane, Ibrahim F. Farag, Shufei Lei, Kari Finstad, Ronald Amundson, Karthik Anantharaman, Jinglei Zhou, Alexander J. Probst, Mary E. Power, Susannah G. Tringe, Wen-Jun Li, Kelly Wrighton, Sue Harrison, Michael Morowitz, David A. Relman, Jennifer A. Doudna, Anne-Catherine Lehours, Lesley Warren, Jamie H. D. Cate, Joanne M. Santini, and Jillian F. Banfield. Clades of huge phages from across Earth’s ecosystems. *Nature*, 578(7795):425–431, February 2020. ISSN 1476-4687. doi: 10.1038/s41586-020-2007-4. URL <https://www.nature.com/articles/s41586-020-2007-4>.
- [11] Teagan L Brown, Oliver J Charity, and Evelien M Adriaenssens. Ecological and functional roles of bacteriophages in contrasting environments: Marine, terrestrial and human gut. *Current Opinion in Microbiology*, 70:102229, December 2022. ISSN 1369-5274. doi: 10.1016/j.mib.2022.102229. URL <https://www.sciencedirect.com/science/article/pii/S1369527422001138>.
- [12] Sandra Chibani-Chennoufi, Anne Bruttin, Marie-Lise Dillmann, and Harald Brüssow. Phage-Host Interaction: An Ecological Perspective. *Journal of Bacteriology*, 186(12):3677–3686, June 2004. ISSN 0021-9193. doi: 10.1128/JB.186.12.3677-3686.2004. URL <https://www.ncbi.nlm.nih.gov/pmc/articles/PMC419959/>.

- [13] Sebastián Coloma, Ursula Gaedke, Kaarina Sivonen, and Teppo Hiltunen. Frequency of virus-resistant hosts determines experimental community dynamics. *Ecology*, 100(1):e02554, 2019. ISSN 1939-9170. doi: 10.1002/ecy.2554. URL <https://onlinelibrary.wiley.com/doi/abs/10.1002/ecy.2554>.
- [14] Stephen Tucker and Peter Pollard. Identification of Cyanophage Ma-LBP and Infection of the Cyanobacterium *Microcystis aeruginosa* from an Australian Subtropical Lake by the Virus. *Applied and Environmental Microbiology*, 71(2):629–635, February 2005. doi: 10.1128/AEM.71.2.629-635.2005. URL <https://journals.asm.org/doi/10.1128/aem.71.2.629-635.2005>.
- [15] Stephen Odonkor and Kennedy Addo. Bacteria Resistance to Antibiotics: Recent Trends and Challenges. *International Journal of Biological & Medical Research*, pages 1204–1210, January 2011.
- [16] Angelina Volkova, Kelly Ruggles, Anjelique Schulfer, Zhan Gao, Stephen D. Ginsberg, and Martin J. Blaser. Effects of early-life penicillin exposure on the gut microbiome and frontal cortex and amygdala gene expression. *iScience*, 24(7):102797, July 2021. ISSN 2589-0042. doi: 10.1016/j.isci.2021.102797. URL <https://www.ncbi.nlm.nih.gov/pmc/articles/PMC8324854/>.
- [17] Nana Nguefang Laure and Juhee Ahn. Phage resistance-mediated trade-offs with antibiotic resistance in *Salmonella* Typhimurium. *Microbial Pathogenesis*, 171:105732, October 2022. ISSN 08824010. doi: 10.1016/j.micpath.2022.105732. URL <https://linkinghub.elsevier.com/retrieve/pii/S088240102200345X>.
- [18] Yuanyang Zhao, Mei Shu, Ling Zhang, Chan Zhong, Ningbo Liao, and Guoping Wu. Phage-driven coevolution reveals trade-off between antibiotic and phage resistance in *Salmonella* anatum. *ISME Communications*, 4(1):ycae039, January 2024. ISSN 2730-6151. doi: 10.1093/ismeco/ycae039. URL <https://doi.org/10.1093/ismeco/ycae039>.
- [19] Beata Kowalska. Fresh vegetables and fruit as a source of *Salmonella* bacteria. *Annals of agricultural and environmental medicine: AAEM*, 30(1):9–14, March 2023. ISSN 1898-2263. doi: 10.26444/aaem/156765.
- [20] Zongcheng Li. Exploring complicated behaviors of a delay differential equation. *Mathematical Modelling and Control*, 3(mmc-03-01-001):1–6, 2023. ISSN 2767-8946. doi: 10.3934/mmc.2023001. URL <http://www.aimspress.com/article/doi/10.3934/mmc.2023001>.
- [21] Yuncong Geng, Thu Vu Phuc Nguyen, Ehsan Homaei, and Ido Golding. Using bacterial population dynamics to count phages and their lysogens. *Nature*

- Communications*, 15(1):7814, September 2024. ISSN 2041-1723. doi: 10.1038/s41467-024-51913-6. URL <https://www.nature.com/articles/s41467-024-51913-6>.
- [22] Meyers Robert A. Encyclopedia of Physical Science and Technology. URL <http://www.sciencedirect.com:5070/referencework/9780122274107/encyclopedia-of-physical-science-and-technology>.
- [23] Edel Stone, Katrina Campbell, Irene Grant, and Olivia McAuliffe. Understanding and Exploiting Phage–Host Interactions. *Viruses*, 11(6):567, June 2019. ISSN 1999-4915. doi: 10.3390/v11060567. URL <https://www.ncbi.nlm.nih.gov/pmc/articles/PMC6630733/>.
- [24] Dalton V. Banh, Cameron G. Roberts, Adrian Morales-Amador, Brandon A. Berryhill, Waqas Chaudhry, Bruce R. Levin, Sean F. Brady, and Luciano A. Marraffini. Bacterial cGAS senses a viral RNA to initiate immunity. *Nature*, 623(7989):1001–1008, November 2023. ISSN 1476-4687. doi: 10.1038/s41586-023-06743-9. URL <https://www.nature.com/articles/s41586-023-06743-9>.
- [25] Joanna Warwick-Dugdale, Holger H. Buchholz, Michael J. Allen, and Ben Temper-ton. Host-hijacking and planktonic piracy: How phages command the microbial high seas. *Virology Journal*, 16(1):1–13, December 2019. ISSN 1743-422X. doi: 10.1186/s12985-019-1120-1. URL <https://virologyj.biomedcentral.com/articles/10.1186/s12985-019-1120-1>.
- [26] Asaf Levy, Moran G. Goren, Ido Yosef, Oren Auster, Miriam Manor, Gil Amitai, Rotem Edgar, Udi Qimron, and Rotem Sorek. CRISPR adaptation biases explain preference for acquisition of foreign DNA. *Nature*, 520(7548):505–510, April 2015. ISSN 1476-4687. doi: 10.1038/nature14302. URL <https://www.nature.com/articles/nature14302>.
- [27] P. M. Sharp. Molecular evolution of bacteriophages: Evidence of selection against the recognition sites of host restriction enzymes. *Molecular Biology and Evolution*, 3(1):75–83, January 1986. ISSN 0737-4038. doi: 10.1093/oxfordjournals.molbev.a040377.
- [28] Matthew K Waldor and David I Friedman. Phage regulatory circuits and virulence gene expression. *Current Opinion in Microbiology*, 8(4):459–465, August 2005. ISSN 1369-5274. doi: 10.1016/j.mib.2005.06.001. URL <https://www.sciencedirect.com/science/article/pii/S1369527405000755>.
- [29] Louis-Charles Fortier and Ognjen Sekulovic. Importance of prophages to evolution and virulence of bacterial pathogens. *Virulence*, 4(5):354–365, July 2013. ISSN

- 2150-5594. doi: 10.4161/viru.24498. URL <https://www.ncbi.nlm.nih.gov/pmc/articles/PMC3714127/>.
- [30] Anastasia A. Aksyuk and Michael G. Rossmann. Bacteriophage Assembly. *Viruses*, 3(3):172–203, February 2011. ISSN 1999-4915. doi: 10.3390/v3030172. URL <https://www.ncbi.nlm.nih.gov/pmc/articles/PMC3185693/>.
- [31] I. N. Wang, D. L. Smith, and R. Young. Holins: The protein clocks of bacteriophage infections. *Annual Review of Microbiology*, 54:799–825, 2000. ISSN 0066-4227. doi: 10.1146/annurev.micro.54.1.799.
- [32] Claudia Igler. Phenotypic flux: The role of physiology in explaining the conundrum of bacterial persistence amid phage attack. *Virus Evolution*, 8(2):veac086, July 2022. ISSN 2057-1577. doi: 10.1093/ve/veac086. URL <https://doi.org/10.1093/ve/veac086>.
- [33] Richard E Lenski. TWO-STEP RESISTANCE BY ESCHERICHIA COLI B TO BACTERIOPHAGE T2. *Genetics*, 107(1):1–7, May 1984. ISSN 1943-2631. doi: 10.1093/genetics/107.1.1. URL <https://doi.org/10.1093/genetics/107.1.1>.
- [34] Sanju Tamang. Horizontal Gene Transfer in Prokaryotes and Eukaryotes, September 2023. URL <https://microbenotes.com/horizontal-gene-transfer-prokaryotes-eukaryotes/>.
- [35] Laura M. Kasman and La Donna Porter. Bacteriophages. In *StatPearls*. StatPearls Publishing, Treasure Island (FL), 2025. URL <http://www.ncbi.nlm.nih.gov/books/NBK493185/>.
- [36] Demeng Tan, Sine Lo Svenningsen, and Mathias Middelboe. Quorum Sensing Determines the Choice of Antiphage Defense Strategy in *Vibrio anguillarum*. *mBio*, 6(3):10.1128/mbio.00627–15, June 2015. doi: 10.1128/mbio.00627-15. URL <https://journals.asm.org/doi/10.1128/mbio.00627-15>.
- [37] Avinoam Rabinovitch, Ira Aviram, and Arie Zaritsky. Bacterial debris—an ecological mechanism for coexistence of bacteria and their viruses. *Journal of Theoretical Biology*, 224(3):377–383, October 2003. ISSN 0022-5193. doi: 10.1016/S0022-5193(03)00174-7. URL <https://www.sciencedirect.com/science/article/pii/S0022519303001747>.
- [38] James J. Bull, Kelly A. Christensen, Carly Scott, Benjamin R. Jack, Cameron J. Crandall, and Stephen M. Krone. Phage-Bacterial Dynamics with Spatial Structure: Self Organization around Phage Sinks Can Promote Increased Cell Densities. *Antibiotics*, 7(1):8, March 2018. ISSN 2079-6382. doi: 10.3390/antibiotics7010008. URL <https://www.mdpi.com/2079-6382/7/1/8>.

- [39] Anika Gupta, Norma Morella, Dmitry Sutormin, Naisi Li, Karl Gaisser, Alexander Robertson, Yaroslav Ispolatov, Georg Seelig, Neelendu Dey, and Anna Kuchina. Combinatorial phenotypic landscape enables bacterial resistance to phage infection, January 2025. URL <https://www.biorxiv.org/content/10.1101/2025.01.13.632860v1>.
- [40] Stephen T. Abedon. Phage “delay” towards enhancing bacterial escape from biofilms: A more comprehensive way of viewing resistance to bacteriophages. *AIMS Microbiology*, 3(microbiol-03-00186):186–226, 2017. ISSN 2471-1888. doi: 10.3934/microbiol.2017.2.186. URL <http://www.aimspress.com/article/doi/10.3934/microbiol.2017.2.186>.
- [41] Rasmus Skytte Eriksen, Sine L. Svenningsen, Kim Sneppen, and Namiko Mitarai. A growing microcolony can survive and support persistent propagation of virulent phages. *Proceedings of the National Academy of Sciences*, 115(2):337–342, January 2018. ISSN 0027-8424, 1091-6490. doi: 10.1073/pnas.1708954115. URL <https://pnas.org/doi/full/10.1073/pnas.1708954115>.
- [42] Christoph Lohrmann, Christian Holm, and Sujit S. Datta. Influence of bacterial swimming and hydrodynamics on attachment of phages. *Soft Matter*, 20(24):4795–4805, June 2024. ISSN 1744-6848. doi: 10.1039/D4SM00060A. URL <https://pubs.rsc.org/en/content/articlelanding/2024/sm/d4sm00060a>.
- [43] S. Moineau. Bacteriophage. In Stanley Maloy and Kelly Hughes, editors, *Brenner’s Encyclopedia of Genetics (Second Edition)*, pages 280–283. Academic Press, San Diego, January 2013. ISBN 978-0-08-096156-9. doi: 10.1016/B978-0-12-374984-0.00131-5. URL <https://www.sciencedirect.com/science/article/pii/B9780123749840001315>.
- [44] J. J. Bull. Optimality models of phage life history and parallels in disease evolution. *Journal of Theoretical Biology*, 241(4):928–938, August 2006. ISSN 0022-5193. doi: 10.1016/j.jtbi.2006.01.027. URL <https://www.sciencedirect.com/science/article/pii/S0022519306000415>.
- [45] Pramalkumar H. Patel, Véronique L. Taylor, Chi Zhang, Landon J. Getz, Alexa D. Fitzpatrick, Alan R. Davidson, and Karen L. Maxwell. Anti-phage defence through inhibition of virion assembly. *Nature Communications*, 15(1):1644, February 2024. ISSN 2041-1723. doi: 10.1038/s41467-024-45892-x. URL <https://www.nature.com/articles/s41467-024-45892-x>.
- [46] Michael J. Bucher and Daniel M. Czyż. Phage against the Machine: The SIE-ence of Superinfection Exclusion. *Viruses*, 16(9):1348, August 2024. ISSN 1999-4915. doi: 10.3390/v16091348.

- [47] Shuji Kanamaru, Kazuya Uchida, Mai Nemoto, Alec Fraser, Fumio Arisaka, and Petr G. Leiman. Structure and Function of the T4 Spackle Protein Gp61.3. *Viruses*, 12(10):1070, September 2020. ISSN 1999-4915. doi: 10.3390/v12101070. URL <https://www.ncbi.nlm.nih.gov/pmc/articles/PMC7650644/>.
- [48] Justin C. Leavitt, Brianna M. Woodbury, Eddie B. Gilcrease, Charles M. Bridges, Carolyn M. Teschke, and Sherwood R. Casjens. Bacteriophage P22 SieA-mediated superinfection exclusion. *mBio*, 15(2):e02169–23, January 2024. doi: 10.1128/mbio.02169-23. URL <https://journals.asm.org/doi/10.1128/mbio.02169-23>.
- [49] Portia Mira, Pamela Yeh, and Barry G. Hall. Estimating microbial population data from optical density. *PLOS ONE*, 17(10):e0276040, October 2022. ISSN 1932-6203. doi: 10.1371/journal.pone.0276040. URL <https://journals.plos.org/plosone/article?id=10.1371/journal.pone.0276040>.
- [50] Advanced Wastewater Modelling | GPS-X - Hydromantis. URL <https://www.hydromantis.com/GPSX-innovative.html>.
- [51] Jacqueline Heard, Emma Harvey, Bruce B. Johnson, John D. Wells, and Michael J. Angove. The effect of filamentous bacteria on foam production and stability. *Colloids and Surfaces. B, Biointerfaces*, 63(1):21–26, May 2008. ISSN 0927-7765. doi: 10.1016/j.colsurfb.2007.10.011.
- [52] Brendan J. M. Bohannan and Richard E. Lenski. Effect of Resource Enrichment on a Chemostat Community of Bacteria and Bacteriophage. *Ecology*, 78(8):2303–2315, 1997. ISSN 1939-9170. doi: 10.1890/0012-9658(1997)078[2303:EOREOA]2.0.CO;2. URL <https://onlinelibrary.wiley.com/doi/abs/10.1890/0012-9658%281997%29078%5B2303%3AEOREOA%5D2.0.CO%3B2>.
- [53] Richard E. Lenski. Dynamics of Interactions between Bacteria and Virulent Bacteriophage. In K. C. Marshall, editor, *Advances in Microbial Ecology*, pages 1–44. Springer US, Boston, MA, 1988. ISBN 978-1-4684-5409-3. doi: 10.1007/978-1-4684-5409-3_1. URL https://doi.org/10.1007/978-1-4684-5409-3_1.
- [54] Pauli Virtanen, Ralf Gommers, Travis E. Oliphant, Matt Haberland, Tyler Reddy, David Cournapeau, Evgeni Burovski, Pearu Peterson, Warren Weckesser, Jonathan Bright, Stéfan J. van der Walt, Matthew Brett, Joshua Wilson, K. Jarrod Millman, Nikolay Mayorov, Andrew R. J. Nelson, Eric Jones, Robert Kern, Eric Larson, C. J. Carey, İlhan Polat, Yu Feng, Eric W. Moore, Jake VanderPlas, Denis Laxalde, Josef Perktold, Robert Cimrman, Ian Henriksen, E. A. Quintero, Charles R. Harris, Anne M. Archibald, Antônio H. Ribeiro, Fabian Pedregosa, and Paul van Mulbregt. SciPy 1.0: Fundamental algorithms for scientific computing in Python.

- Nature Methods*, 17(3):261–272, March 2020. ISSN 1548-7105. doi: 10.1038/s41592-019-0686-2. URL <https://www.nature.com/articles/s41592-019-0686-2>.
- [55] J. R. Dormand and P. J. Prince. A family of embedded Runge-Kutta formulae. *Journal of Computational and Applied Mathematics*, 6(1):19–26, March 1980. ISSN 0377-0427. doi: 10.1016/0771-050X(80)90013-3. URL <https://www.sciencedirect.com/science/article/pii/0771050X80900133>.
- [56] Dash Documentation & User Guide | Plotly. URL <https://dash.plotly.com/>.
- [57] Dask Development Team. *Dask: Library for dynamic task scheduling*, 2016. URL <http://dask.pydata.org>.
- [58] Python Software Foundation. Python programming language, version 3.11.6, 2024. URL <https://www.python.org>. Accessed: 2025-05-19.
- [59] Charles R. Harris, K. Jarrod Millman, Stéfan J. van der Walt, Ralf Gommers, Pauli Virtanen, David Cournapeau, Eric Wieser, Julian Taylor, Sebastian Berg, Nathaniel J. Smith, Robert Kern, Matti Picus, Stephan Hoyer, Marten H. van Kerkwijk, Matthew Brett, Allan Haldane, Jaime Fernández del Río, Mark Wiebe, Pearu Peterson, Pierre Gérard-Marchant, Kevin Sheppard, Tyler Reddy, Warren Weckesser, Hameer Abbasi, Christoph Gohlke, and Travis E. Oliphant. Array programming with NumPy. *Nature*, 585(7825):357–362, September 2020. doi: 10.1038/s41586-020-2649-2. URL <https://doi.org/10.1038/s41586-020-2649-2>.
- [60] Takuya Iwanaga, William Usher, and Jonathan Herman. Toward SALib 2.0: Advancing the accessibility and interpretability of global sensitivity analyses. *Socio-Environmental Systems Modelling*, 4:18155–18155, May 2022. ISSN 2663-3027. doi: 10.18174/sesmo.18155. URL <https://sesmo.org/article/view/18155>.
- [61] Jon Herman and Will Usher. SALib: An open-source Python library for Sensitivity Analysis. *Journal of Open Source Software*, 2(9):97, January 2017. ISSN 2475-9066. doi: 10.21105/joss.00097. URL <https://joss.theoj.org/papers/10.21105/joss.00097>.
- [62] Aric Hagberg, Pieter J. Swart, and Daniel A. Schult. Exploring network structure, dynamics, and function using NetworkX. Technical Report LA-UR-08-05495; LA-UR-08-5495, Los Alamos National Laboratory (LANL), Los Alamos, NM (United States), January 2008. URL <https://www.osti.gov/biblio/960616>.
- [63] J. D. Hunter. Matplotlib: A 2d graphics environment. *Computing in Science & Engineering*, 9(3):90–95, 2007. doi: 10.1109/MCSE.2007.55.

- [64] Lars Fieseler and Steven Hagens. Food Safety. In David R. Harper, Stephen T. Abedon, Benjamin H. Burrowes, and Malcolm L. McConville, editors, *Bacteriophages: Biology, Technology, Therapy*, pages 857–890. Springer International Publishing, Cham, 2021. ISBN 978-3-319-41986-2. doi: 10.1007/978-3-319-41986-2_29. URL https://doi.org/10.1007/978-3-319-41986-2_29.
- [65] Heinz G. Floss and Tin-Wein Yu. Rifamycin Mode of Action, Resistance, and Biosynthesis. *Chemical Reviews*, 105(2):621–632, February 2005. ISSN 0009-2665. doi: 10.1021/cr030112j. URL <https://doi.org/10.1021/cr030112j>.
- [66] A. Tomasz. The Mechanism of the Irreversible Antimicrobial Effects of Penicillins: How the Beta-Lactam Antibiotics Kill and Lyse Bacteria. *Annual Review of Microbiology*, 33(Volume 33, 1979):113–137, October 1979. ISSN 0066-4227, 1545-3251. doi: 10.1146/annurev.mi.33.100179.000553. URL <https://www.annualreviews.org/content/journals/10.1146/annurev.mi.33.100179.000553>.
- [67] Sergei B. Vakulenko and Shahriar Mobashery. Versatility of Aminoglycosides and Prospects for Their Future. *Clinical Microbiology Reviews*, 16(3):430–450, July 2003. doi: 10.1128/cmr.16.3.430-450.2003. URL <https://journals.asm.org/doi/10.1128/cmr.16.3.430-450.2003>.
- [68] Sophie Leclercq, Firoz M. Mian, Andrew M. Stanisz, Laure B. Bindels, Emmanuel Cambier, Hila Ben-Amram, Omry Koren, Paul Forsythe, and John Bienenstock. Low-dose penicillin in early life induces long-term changes in murine gut microbiota, brain cytokines and behavior. *Nature Communications*, 8:15062, April 2017. ISSN 2041-1723. doi: 10.1038/ncomms15062. URL <https://www.ncbi.nlm.nih.gov/pmc/articles/PMC5382287/>.
- [69] Global action plan on antimicrobial resistance. URL <https://www.who.int/publications/i/item/9789241509763>.
- [70] Christopher R. Grasso, Kaytee L. Pokrzywinski, Christopher Waechter, Taylor Rycroft, Yanyan Zhang, Alyssa Aligata, Michael Kramer, and Anisha Lamsal. A Review of Cyanophage–Host Relationships: Highlighting Cyanophages as a Potential Cyanobacteria Control Strategy. *Toxins*, 14(6):385, June 2022. ISSN 2072-6651. doi: 10.3390/toxins14060385. URL <https://www.mdpi.com/2072-6651/14/6/385>.
- [71] Katelyn M. McKindles, Makayla A. Manes, Jonathan R. DeMarco, Andrew McClure, R. Michael McKay, Timothy W. Davis, and George S. Bullerjahn. Dissolved Microcystin Release Coincident with Lysis of a Bloom Dominated by *Microcystis* spp. in Western Lake Erie Attributed to a Novel Cyanophage. *Applied and Environmental Microbiology*, 86(22):e01397–20, October 2020. doi: 10.1128/AEM.01397-20. URL <https://journals.asm.org/doi/10.1128/aem.01397-20>.

- [72] (PDF) Economic Impacts of Red Tide Events on Restaurant Sales. URL https://www.researchgate.net/publication/23515658_Economic_Impacts_of_Red_Tide_Events_on_Restaurant_Sales.
- [73] Yung Sung Cheng, Yue Zhou, Clinton M. Irvin, Richard H. Pierce, Jerome Naar, Lorraine C. Backer, Lora E. Fleming, Barbara Kirkpatrick, and Dan G. Baden. Characterization of Marine Aerosol for Assessment of Human Exposure to Breve-toxins. *Environmental Health Perspectives*, 113(5):638–643, May 2005. ISSN 0091-6765. doi: 10.1289/ehp.7496. URL <https://www.ncbi.nlm.nih.gov/pmc/articles/PMC1257561/>.
- [74] Barbara Kirkpatrick, Judy A Bean, Lora E Fleming, Gary Kirkpatrick, Lynne Grief, Kate Nierenberg, Andrew Reich, Sharon Watkins, and Jerome Naar. Gastrointestinal Emergency Room Admissions and Florida Red Tide Blooms. *Harmful algae*, 9(1):82–86, January 2010. ISSN 1568-9883. doi: 10.1016/j.hal.2009.08.005. URL <https://www.ncbi.nlm.nih.gov/pmc/articles/PMC2786186/>.
- [75] Porter Hoagland, Di Jin, Lara Y. Polansky, Barbara Kirkpatrick, Gary Kirkpatrick, Lora E. Fleming, Andrew Reich, Sharon M. Watkins, Steven G. Ullmann, and Lorraine C. Backer. The costs of respiratory illnesses arising from Florida gulf coast *Karenia brevis* blooms. *Environmental Health Perspectives*, 117(8):1239–1243, August 2009. ISSN 1552-9924. doi: 10.1289/ehp.0900645.